MASS. INST. TECHNOLOGY
JUN 6 1961
LIBRARY

FILM BOILING ON THE INSIDE OF HORIZONTAL TUBES IN FORCED CONVECTION

by

ROBERT ALAN KRUGER

B.S., Massachusetts Institute of Technology (1957)

SUBMITTED IN PARTIAL FULFILLMENT
OF THE REQUIREMENTS FOR THE
DEGREE OF DOCTOR OF
PHILOSOPHY

at the

MASSACHUSETTS INSTITUTE OF
TECHNOLOGY

June, 1961

Signature of Author...
Department of Mechanical Engineering, May 26, 1961

Certified by.............. ......
Thesis Supervisor

Accepted by...
Chairman, Departmental Committee
on Graduate Students

FILM BOILING ON THE INSIDE OF HORIZONTAL TUBES IN FORCED CONVECTION

by

ROBERT A. KRUGER

Submitted to the Department of Mechanical Engineering on May 26, 1961 in partial fulfillment of the requirements for the degree of Doctor of Philosphy.

ABSTRACT

It has been well established that a region of stable film boiling exists when the temperature of a heated surface in contact with a liquid is much higher than the saturation temperature of the liquid. It was the purpose of this investigation to study the mechanism of film boiling for a liquid flowing through a heated tube in forced convection.

Two preliminary experiments were conducted. One of these, in which the heated tube was glass, was used to demonstrate that a stable flow pattern exists. In this experiment it appeared that a thin vapor film formed under the liquid near the tube wall. The vapor produced by the boiling flowed upward near the tube wall and collected in a vapor layer at the top of the tube. The second preliminary experiment was used to estimate the magnitude of the heat transfer coefficient in this type of flow.

A more fully instrumented experiment was designed and operated which allowed the tube wall temperatures, the fluid flow rate and the heat transfer rate to be measured.

In order to treat the problem analytically, it was necessary to estimate the heat transfer coefficient to the liquid and to the vapor layer at the top of the tube. Knowledge of the ratio of the area of the vapor flow to the area of the liquid flow at any cross section was also required.

The heat transfer coefficient for the boiling liquid was calculated in a manner very similar to that developed by Bromley for the film boiling of a liquid on the outside of a rod. The heat transfer coefficient for the vapor at the top of the tube was estimated by ordinary empirical correlations. The area ratio of the flow was estimated by considering the pressure drop in the tube.

Combination of these quantities in a conduction equation for the tube wall allowed a method of calculation to be developed which yields temperature distributions for an electrically heated tube.

The calculated values of the temperature difference between the tube wall and the boiling temperature of the liquid were found to be within ± 15% of the measured values. The theory in its present form underestimates the temperature rise with tube length in most cases.

Thesis Supervisor: Warren M. Rohsenow

Title: Professor of Mechanical Engineering

BIOGRAPHICAL NOTE

The author was born in Oklahoma City, Oklahoma in 1935 and received his early education in the public schools of that city. He attended the University of Oklahoma as a freshman from 1953 to 1954. In 1954 he came to M.I.T. and received the Bachelor of Science Degree in Mechanical Engineering in June 1957. He was a graduate student in the Engineering Department at Cambridge University, England, during the academic year 1957 to 1958. In 1958 he returned to M.I.T. as a graduate student.

The results of the studies undertaken at Cambridge University were published in the report "The Performance of a Cascade Fitted with Blown Flaps", Aeronautical Research Council Report, ARC 21,101-EA695, 23 June 1959.

He was employed as an engineer by the Douglas Aircraft Co., Santa Monica, California during the summer of 1957. He has received the following fellowships: National Science Foundation Fellowships 1957-1958, 1959-1960, 1960-1961; Procter and Gamble Fellowship 1958-1959; Standard Oil Company of California Scholarship 1956-1957.

The author is an associate member of the American Society of Mechanical Engineers. He is also a member of the Society of Sigma Xi, Tau Beta Pi and Pi Tau Sigma.

ACKNOWLEDGEMENTS

Financial support for the investigations reported in this thesis was supplied by a grant from the National Science Foundation.

The members of my thesis committee, Professors Peter Griffith, R. J. Nickerson, S. W. Gouse and Raphael Moissis gave me the benefit of many helpful suggestions and valuable discussions both during thesis committee meetings and individually while the investigations were being carried out.

Mr. E. F. Doyle provided a great deal of assistance in operating the experiment and in performing the calculations.

My wife, Donna, assisted me in many ways throughout the course of the investigations and was particularly helpful in the preparation of this report.

I am deeply indebted to my advisor, Professor Warren M. Rohsenow, whose guidance, assistance and support were most generously given.

TABLE OF CONTENTS

TABLE OF FIGURES

page

I INTRODUCTION

A great deal of work has been done in recent years on the general topic of boiling heat transfer. It has been well established that several distinct regimes of heat transfer occur in the boiling process. Rohsenow (ref. 1) and Westwater (ref. 2) have presented thorough discussions of the various types of boiling.

The type of boiling of most practical importance and most frequently encountered in commercial applications is nucleate boiling. In nucleate boiling high heat transfer rates are obtained with very small temperature differences. Bubbles form on the heated surface, rapidly grow and break away from the surface. The resulting agitation of the liquid near the wall produces high heat transfer coefficients.

The second region of boiling is the transition region. In transition boiling an increase in the temperature difference between the heated surface and the boiling liquid results in a decrease in the heat transfer rate. According to Berenson (ref. 3) transition boiling is a combination of unstable nucleate and unstable film boiling alternating at a single location on the hot surface.

The type of boiling that is of interest in this report is film boiling. In stable film boiling the liquid does not wet the heated surface but is separated from it by a thin vapor film. This type of boiling is characterized by very large temperature differences between the heated surface and the boiling liquid.

Stable film boiling has been observed and photographed on external geometries by several investigators. See, for example, Ellion (ref.4) or Bromley (ref. 5). Bromley derived an analytical method of predicting heat transfer coefficients on a horizontal rod in natural convection. In a later paper Bromley (ref. 6) discussed film boiling on a horizontal rod in forced convection, obtaining results similar to those for natural convection. He also treated analytically the case of film boiling on the outside of a vertical rod.

Hsu and Westwater (ref. 7) found experimentally that Bromley's equation for the heat transfer on vertical surfaces predicted values of the heat transfer coefficient which were too low. The same authors (ref. 8) later developed an analysis which partially explained the difference between Bromley's equation and the data in terms of turbulence developing in the natural convection boundary layer.

Laminar forced convection film boiling has been treated on external geometries by Bradfield (ref. 9) and Cess and Sparrow (ref. 10) by considering the growth of a laminar vapor boundary layer.

Film boiling in flows of cryogenic fluids has recently been investigated by Graham (ref. 11) and von Glahn (ref. 12). These studies were conducted on the inside of vertical tubes with high outlet vapor qualities. Sterman and Styshen (ref. 13) have also indicated that film boiling on the inside of tubes has been observed. Their studies were concerned with maximum and minimum heat flux.

The general problem investigated in this report has been film boiling on the inside of tubes in forced convection. This case was found to be quite different from the forced convection boundary layer flow considered by Cess and Sparrow (ref. 10) but quite similar to the flow observed by Bromley (ref. 5). In a horizontal tube the vapor produced by the boiling will not be entrained in a vapor boundary layer which increases in thickness as the distance down the tube increases but the vapor will collect at the top of the tube and form a stratified flow. The qualitative nature of the flow considered here is shown in Figure 1 and Figure 7.

The object of the present experimental program was to relate the values of temperature of the tube wall to the heat transfer rate and the velocity of the liquid in the tube. Provisions were made in the apparatus to maintain the flow of liquid entering the heated tube at near saturation temperature at low pressure (near atmospheric). The tube dimensions and heat transfer rates used in the tests were such that the mass flow rate of vapor at the outlet of the heated tube was small compared to the total mass flow rate.

The object of the theoretical program was to develop an idealized flow model from which it would be possible to calculate the temperature of the tube wall for a given flow of a known fluid and a given heat transfer rate. The area of interest in the analysis was where the mass flow of vapor was small compared to the total mass flow in the tube.

Film boiling is of interest in many areas. In general the development of film boiling is possible in the operation of equipment in which the heat input is the controlled quantity. The possibility of an abrupt temperature rise in the operation of atomic power plants, for example, should be considered in their design.

Another region of great interest is the flow of cryogenic fluids. Since the saturation temperatures of cryogenic fluids are extremely low, film boiling may occur when the fluid flows over surfaces at ordinary temperatures. The extensive use of this type of fluid as fuel in rocket engines causes a large area of possible use of a study of film boiling on the inside of tubes. Finally, the process of film boiling on the inside of tubes in continuous operation might find application as a temperature control device at high temperature levels.

II THEORETICAL PROGRAM

A. Introduction

The object of this analysis has been to predict the temperature distribution along the length of a heated tube in which a liquid is boiling in the film boiling regime in forced convection. Visual observation of the flow pattern in a preliminary experiment suggested the basic model for the analysis. The geometry that was considered is shown in Figure 7. The idealized boiling process is quite similar to that analyzed by Bromley (ref. 5) where he considered film boiling in natural convection on the outside of a cylindrical rod.

It was assumed that a stable vapor film develops near the hot tube wall which supports the liquid flow above it. The vapor produced by the boiling flows upward near the tube wall under the action of bouyant forces and collects in a v or layer at the top of the tube. The analysis done here is restricted to the region in which the mass flow of vapor at the tube outlet is small compared to the total mass flow. The region in which the assumption of primary stratified flow is valid has not been defined. It might be noted, however, that stratified flow was observed in the heated section of the visual test section while bubble flow was observed downstream from the heated section of the tube. That is, the usual correlation for two phase flow patterns may not be valid for the accelerating flow in the film boiling process. It would seem reasonable for this model to break down when the mass flow of vapor becomes large.

An expression for the average film boiling heat transfer coefficient around a horizontal rod was derived by Bromley (ref. 5). The primary assumptions in his analysis were that the bouyant forces in the vapor film cause the vapor to flow upward around the tube, that the flow in the vapor film is laminar and that the liquid-vapor interface is smooth. The analysis yields, in its simplest form, the following expression for the heat transfer coefficient in the absence of radiation.

$$h_{co} = (\text{const.})\left\{\frac{K_v^3 \rho_v(\rho_L - \rho_v) g \lambda'}{D \mu_v \Delta T}\right\}^{1/4} \qquad \text{(II-1)}$$

It will be shown later that the expression used for the boiling heat transfer coefficient in this analysis is exactly the same as that in equation (II-1) but written in a slightly different form.

The present analysis is concerned with the flow on the inside of a tube. In this case the vapor produced by the boiling is not free to escape as it is for boiling on external surfaces but must collect in the tube and flow axially downstream with the liquid. The amount of vapor in the flow will thus be different at each position along the tube and a variation of tube wall temperature with length may be expected. For this reason it was decided to rewrite equation (II-1) using the heat transfer rate as the independent variable rather than the temperature difference. Another difference in the average boiling heat transfer coefficient is caused by the vapor layer at the top of the tube. Figure 7 shows that the boiling occurs only over a part of the tube circumference. Since the heat transfer coefficient is a function of the angle θ it was necessary to find an averaging factor which would account for the variation of boiling surface area with tube length.

B. Determination of the heat transfer coefficient across the thin vapor film.

For the geometry shown in Figure 7, if laminar flow in the tangential direction in the vapor film is assumed and momentum changes neglected, the following equations may be written.

For control volume A

$$\frac{\partial p}{\partial \theta} = -\rho_L g \frac{D}{2} \sin\theta \tag{II-2}$$

For control volume B

$$\frac{\partial p}{\partial \theta} = -\rho_v g \frac{D}{2} \sin\theta - (\tau_w)_T \frac{D}{2b} \tag{II-3}$$

$(\tau_w)_T$ represents the total shearing stress acting on the vapor flow, both from the tube wall and from the liquid-vapor interface. Bromley (ref. 5) calculated the frictional forces for the two extreme cases where the liquid was either considered rigid or completely frictionless. The actual drag force should be within these two limits. The effect on the heat transfer coefficient of the evaluation of friction drag appears as a coefficient which varies between fixed limits. Bromley determined this coefficient experimentally.

A full derivation of the shearing stress term is included in Appendix A. Since the derivation of the local boiling heat transfer coefficient follows Bromley's method very closely, the discussion here will be brief.

The heat transfer across the vapor film is composed of two parts, convection and radiation. The heat transfer by radiation produces boiling at the liquid surface in addition to that produced by convection. The rate of formation of vapor per unit area must then be written as

$$\frac{dw_{vs}}{dx} = \frac{(q/A)_T}{\lambda'} \qquad \text{(II-4)}$$

where $(q/A)_T$ is the total heat transfer rate, the sum of radiation and convection. λ' is the average heat content of the vapor above that of saturated liquid. The evaluation of the vapor heat content is discussed in Appendix B.

If laminar flow in the vapor film is assumed and equation (II-4) is used to find the vapor flow rate, the wall shearing stress can be evaluated as

$$(\tau_w)_T = -(\text{const.})\,\frac{\mu_v (q/A)_T \frac{D}{2}\,\theta}{\rho_v\, b^2\, \lambda'} \qquad \text{(II-5)}$$

The constant assumes the value 3 for the case of no drag at the liquid-vapor interface and the value 12 when the liquid is considered to be rigid.

Combining equations (II-2), (II-3) and (II-5) gives the following expression for the thickness of the vapor film.

$$b = \beta' \left\{ \frac{\mu_v (q/A)_T D}{\rho_v (\rho_L - \rho_v) g \lambda'} \right\}^{1/3} \left\{ \frac{\theta}{\sin\theta} \right\}^{1/3} \tag{II-6}$$

The value of β' is to be determined according to the final choice of velocity profiles within the limits.

$$3 \leq 2(\beta')^3 \leq 12 \tag{II-7}$$

If a linear temperature distribution in the vapor film is assumed, the local boiling heat transfer coefficient may be written as

$$h_{LB} = K_v/b = \frac{(q/A)_c}{\Delta T} \tag{II-8}$$

or

$$h_{LB} = \frac{1}{\beta'} \left\{ \frac{K_v^3 \rho_v (\rho_L - \rho_v) g \lambda'}{D \mu_v (q/A)_T} \right\}^{1/3} \left\{ \frac{\sin\theta}{\theta} \right\}^{1/3} \tag{II-9}$$

Using equation (II-9), the average value of the heat transfer coefficient in the boiling region can be determined by a graphical integration. That is,

$$\bar{h}_{LB} = \frac{1}{(\pi - \alpha)} \int_0^{(\pi-\alpha)} h_{LB}\, d\theta \tag{II-10}$$

Equation (II-10) can be expressed in the following form where the coefficient γ is the result of the integration. This averaging factor is plotted as a function of the interface angle in Figure 10.

$$\bar{h}_{LB} = \frac{\gamma}{\beta'}\left\{\frac{K_v^3 \rho_v(\rho_L - \rho_v) g \lambda'}{D \mu_v (q/A)_T}\right\}^{1/3} \tag{II-11}$$

In the absence of radiation the total heat flux can be expressed as

$$(q/A)_T = \bar{h}_{LB} \Delta T \tag{II-12}$$

Substitution of equation (II-12) into equation (II-11) yields the same expression for the boiling heat transfer coefficient as equation (II-1).

C. <u>Determination of the ratio of vapor area to liquid area at any cross section</u>.

In order to estimate the temperature of the tube the area ratio of vapor to liquid must be known as a function of the position along the tube. In these calculations it has been assumed that the mass flow of vapor is small compared to the total mass flow. The geometry of Figure 7 gives

$$A_T = \frac{\pi}{4} D^2 \tag{II-13a}$$

$$A_V = \frac{\pi}{4} D^2 \left(\frac{\alpha}{\pi} - \frac{1}{2\pi} \sin 2\alpha \right) \qquad \text{(II-13b)}$$

$$A_L = \frac{\pi}{4} D^2 \left[1 - \left(\frac{\alpha}{\pi} - \frac{1}{2\pi} \sin 2\alpha \right) \right] \qquad \text{(II-13c)}$$

Since the mass flow of liquid is approximately the total mass flow, the velocity of the liquid is

$$V_L = \frac{\omega_T}{\rho_L A_L} = V_0 \left[1 - \left(\frac{\alpha}{\pi} - \frac{1}{2\pi} \sin 2\alpha \right) \right]^{-1} \qquad \text{(II-14)}$$

The total mass flow of vapor is the total heat input divided by the average heat content of the vapor. Using equation (II-13b) the velocity of the vapor may be found.

$$V_V = \frac{\omega_V}{\rho_V A_V} = \frac{4\left(\overline{q/A}\right) x}{\rho_V \lambda' D} \; \frac{1}{\left(\frac{\alpha}{\pi} - \frac{1}{2\pi} \sin 2\alpha \right)} \qquad \text{(II-15)}$$

Momentum equations were written for the control volumes shown in Figure 8 in order to determine the variation of the interface angle with position along the tube. The pressure gradient in both the liquid layer and the vapor layer can be expressed as a function of friction forces and momentum changes. The two values of the pressure gradient must be equal in order to maintain continuity of pressure across the horizontal liquid-vapor interface. The two momentum equations are

$$-\left(\frac{\partial p}{\partial x}\right)_v A_v - \tau_i D \sin\alpha - (\tau_w)_v \alpha D = \frac{\partial}{\partial x}(\omega_v V_v) - V_L \frac{d\omega_{vB}}{dx} \quad \text{(II-16)}$$

and

$$-\left(\frac{\partial p}{\partial x}\right)_L A_L - (\tau_w)_L (\pi - \alpha) D + \tau_i D \sin\alpha = \frac{\partial}{\partial x}(\omega_L V_L) + V_L \frac{d\omega_{vB}}{dx} \quad \text{(II-17)}$$

These equations were reduced to a useful form by the following substitutions. The shearing stress at the tube wall in contact with the vapor layer and the shear at the horizontal liquid-vapor interface were estimated in terms of friction factors. The shearing stress at the bottom of the tube acting on the liquid was estimated by calculating the shear in the vapor film. A linear axial velocity profile in the vapor film was assumed. Equations (II-18) show the form of these substitutions.

$$(\tau_w)_v = \frac{f}{8} \rho_v V_v^2 \quad \text{(II-18a)}$$

$$\tau_i = \frac{f}{8} \rho_v (V_v - V_L)^2 \quad \text{(II-18b)}$$

$$(\tau_w)_L = \frac{\mu_v V_L}{b} \quad \text{(II-18c)}$$

$$\frac{d\omega_{vB}}{dx} = \frac{(\overline{2/A})\pi D}{\lambda'} \quad \text{(II-18d)}$$

$$V_L = \frac{\omega_L}{\rho_L A_L} \tag{II-18e}$$

$$V_v = \frac{\omega_v}{\rho_v A_v} \tag{II-18f}$$

$$A_v = A_T - A_L \tag{II-18g}$$

Subtracting equation (II-16) from equation (II-17) and substituting equations (II-18) yields

$$\frac{f}{8}\frac{\omega_v^2 D}{\rho_v A_v^3}\left\{\alpha + \sin\alpha\left(1 - \frac{\omega_L \rho_v A_v}{\omega_v \rho_L A_L}\right)^2\left(\frac{A_v}{A_L} + 1\right)\right\} - \frac{\mu_v \omega_L (\pi - \alpha) D}{b \rho_L A_L^2} \tag{II-19}$$

$$= \left\{-\frac{\omega_L^2}{\rho_L A_L^3} - \frac{\omega_v^2}{\rho_v A_v^3}\right\}\frac{\partial A_L}{\partial x} + \frac{\omega_L}{\rho_L A_L^2}\frac{d\omega_{vB}}{dx}\left\{\frac{A_L}{A_v} - 2\frac{\omega_v \rho_L A_L^2}{\omega_L \rho_v A_v^2} - 1\right\}$$

In the region of interest in this paper, particularly where the mass flow of vapor is small compared to the total mass flow, it was found that all friction terms could be omitted from equation (II-19). It was also found that the important momentum terms were the momentum change in the liquid caused by the area change and the momentum change in the vapor caused by the addition of vapor by the boiling. For larger vapor flow rates the friction on the vapor at the top of the tube has increasing importance.

The magnitudes of the various terms were estimated on the basis of values encountered in the experimental program. The assumptions made in this calculation are not necessarily true in general but only for conditions similar to those in the experiments. The primary restriction on the omission of these terms is that the mass rate of flow of vapor must be small compared to the total mass flow. Since this is a limitation of the entire analysis, it seems a reasonable assumption at this point.

Equation (II-19) may be written in the following form if these terms are neglected.

$$\frac{\partial A_L}{\partial x} = -2\,\frac{\omega_v}{\omega_L^2}\,\frac{d\omega_v}{dx}\cdot\frac{\rho_L}{\rho_v}\,\frac{A_L^3}{A_v^2} \qquad \text{(II-20)}$$

Substituting equations (II-18d) and (II-18g) into (II-20) and integrating from zero to x gives

$$\left\{\frac{A_T^2}{A_L^2} - 4\,\frac{A_T}{A_L} + 2\ln\frac{A_T}{A_L} - 3\right\} = 2\left\{\frac{4\,(\overline{q/A})}{\rho_L V_0 \lambda'}\right\}^2 \frac{\rho_L}{\rho_v}\,\frac{x^2}{D^2} \qquad \text{(II-21)}$$

If X_m is defined as

$$X_m = \frac{4\sqrt{2}\,(\overline{q/A})\,x}{\sqrt{\rho_L \rho_V}\,V_0\,\lambda' D} \tag{II-22}$$

use of equations (II-13a) and (II-13c) allows equation (II-21) to be written in the following form.

$$X_m = f\left(\frac{\alpha}{\pi}\right) \tag{II-23}$$

This relation is cumbersome and hard to use in calculations. Figure 11 shows the function defined by equations (II-21), (II-22) and (II-13). This graphical representation was used in the calculation of the interface angle.

D. Estimation of the heat transfer coefficient for the vapor flow.

An estimation of the heat transferred directly to the vapor at the top of the tube must be made in order to completely define the conditions. The method used here is not an accurate one but should give a reasonable estimate of the magnitude and variation of the local vapor heat transfer coefficient. The ordinary correlation for heat transfer data has been used in the following form.

$$\frac{h_{LV} D}{K_b} = 0.023\left(\frac{DG}{\mu_b}\right)^{0.8}\left(\frac{C_p \mu}{K}\right)_b^{0.4} \tag{II-24}$$

The subscript b refers to the evaluation of the properties at the bulk temperature. The Reynolds number may be evaluated by using equation (II-15) and introducing the concept of hydraulic or equivalent diameter. That is,

$$D_e = 4\,\frac{\text{cross sectional area}}{\text{wetted perimeter}} \tag{II-25}$$

The cross sectional area and the wetted perimeter of the vapor flow may be determined as functions of the interface angle from the geometry shown in Figure 7. These relations yield

$$D_e = D\left\{\frac{\alpha/\pi - \frac{1}{2\pi}\sin 2\alpha}{\alpha/\pi + \frac{1}{\pi}\sin\alpha}\right\} \tag{II-26}$$

and

$$\left(\frac{DG}{\mu_b}\right) = \frac{4(\overline{Q/A})x}{\mu_{vb}\,\lambda'}\left\{\frac{1}{\alpha/\pi + \frac{1}{\pi}\sin\alpha}\right\} \tag{II-27}$$

Substitution of equations (II-26) and (II-27) into (II-24) gives a dimensional equation for the local vapor heat transfer coefficient in the following form.

$$h_{Lv} = 0.023\,\frac{K_{vb}}{D}\left(\frac{4(\overline{Q/A})x}{\mu_{vb}\,\lambda'}\right)^{0.8}\left(\frac{C_p\mu}{K}\right)_b^{0.4}\frac{(\alpha/\pi + \frac{1}{\pi}\sin\alpha)^{0.2}}{(\alpha/\pi - \frac{1}{2\pi}\sin 2\alpha)} \tag{II-28}$$

E. Analysis of conduction in the tube wall.

If the heat transfer coefficient for the vapor flow is significantly different from the boiling heat transfer coefficient, it is possible that there will be a substantial temperature difference between the top of the tube and the bottom of the tube. If this is the case, it is necessary to consider the effect of conduction in the tube wall. This analysis is quite similar to that used to calculate the temperature distribution on a finned surface.

The tube considered in this case is one which is heated electrically; that is with a substantially uniform generation of heat per unit volume. Figure 9 shows the geometry used in this analysis. For the purpose of this calculation it will be assumed that the heat transfer coefficient across the thin vapor film in the boiling region may be represented by the mean local boiling coefficient given by equation (II-11). In fact the boiling heat transfer coefficient is a function of the angle from the bottom of the tube. However, the variation is weak except in the region near the top of the tube. Since the vapor flow fills the top of the tube the error introduced by this approximation will be small.

At the top of the tube the heat transfer coefficient, h_{lv}, will be given by equation (II-28). The heat transfer coefficients on the tube surfaces can be written as

$$\left.\begin{aligned} h_{inside} &= \bar{h}_{lb} \\ h_{outside} &= 0 \end{aligned}\right\} \quad 0 \leq \theta \leq (\pi - \alpha)$$

(II-29)

$$\left.\begin{aligned} h_{inside} &= h_{lv} \\ h_{outside} &= 0 \end{aligned}\right\} \quad (\pi - \alpha) \leq \theta \leq \pi$$

The outside surface of the tube is assumed to be well insulated. Radial temperature gradients have been neglected. The uniform generation of heat per unit volume is given by Q.

$$Q = \bar{q}/tA_s \tag{II-30}$$

Considering a differential element of the tube wall allows the radial heat transfer to be expressed as

$$dq_r = h\,\Delta T\, r\, d\theta\, dx + dq_{RAD} \tag{II-31}$$

An ordinary heat balance on the element of tube wall yields the following differential equation if equations (II-30) and (II-31) are used.

$$\frac{\partial^2 T}{\partial \theta^2} - \frac{hr^2}{K_s t} T = -\frac{hr^2}{K_s t} T_s - \frac{r^2}{K_s t}\left[(\overline{q/A}) - (q/A)_{RAD}\right] \tag{II-32}$$

The definition of the following non-dimensional quantities reduces equation (II-32) to (II-34).

$$\frac{h r^2}{K_s t} = a^2 \qquad \text{(II-33a)}$$

$$(q/A)_c = (\overline{q/A}) - (q/A)_{RAD} \qquad \text{(II-33b)}$$

$$b = \left[T_B + \frac{1}{h}(q/A)_c \right] \qquad \text{(II-33c)}$$

$$\frac{\partial^2 T}{\partial \theta^2} - a^2 T = - a^2 b \qquad \text{(II-34)}$$

These equations describe the temperature distribution either at the top of the tube or at the bottom of the tube in the boiling region. Solutions to equation (II-34) can be determined for each of the regions and the solutions matched on the line $\theta = (\pi - \alpha)$. Considerations of symmetry give the two boundary conditions below.

$$\frac{\partial T}{\partial \theta} = 0 \quad at \quad \theta = 0 \qquad \text{(II-35a)}$$

$$\frac{\partial T}{\partial \theta} = 0 \quad at \quad \theta = \pi \qquad \text{(II-35b)}$$

In order to maintain continuity of temperature and of heat flux at the matching point, the following two conditions are required.

$$T_1 = T_2 \quad \text{at} \quad \theta = (\pi - \alpha) \tag{II-36a}$$

$$\frac{\partial T_1}{\partial \theta} = \frac{\partial T_2}{\partial \theta} \quad \text{at} \quad \theta = (\pi - \alpha) \tag{II-36b}$$

If a and b are independent of θ, the equation may be integrated directly. Unfortunately b is not entirely independent of the angle since it contains the heat transfer by radiation. If the temperature varies around the tube circumference, the radiational effects will also vary. Estimates of the order of magnitude of the radiation show that it has a significant effect on the tube temperature but only amounts to about 10% of the total heat transfer. Thus the error introduced by evaluating the heat transferred by radiation at a mean tube wall temperature will affect the calculation of tube temperature by about 10% of the error in the radiation calculation. This should be much smaller than the error introduced by some of the other approximations in the analysis, primarily the estimation of the local vapor heat transfer coefficient.

Another source of error in the calculation of the radiation is the difficulty in determining the view factor. The vapor film is thin in the boiling region and allows the radiation to be treated as if the tube wall and the liquid were parallel plates. The view factor at the top of the tube is somewhat more difficult to estimate in a useful form. Since the radiation is a minor part of the total heat transfer a very approximate method of evaluating the radiation at the top of the tube has been used. The heat transfer by radiation has been calculated using equation (II-37).

$$\left(q/A\right)_{RAD} = \epsilon_s \sigma \left\{ \overline{T}_{WALL}^{\,4} - T_B^{\,4} \right\} \qquad \text{(II-37)}$$

Use of equation (II-37) will necessarily cause some error in the calculations but it is felt that an approximation of this type is required in order to avoid further complications in the analysis.

Solutions to equation (II-34) can easily be obtained in the following form if both <u>a</u> and <u>b</u> are constant.

$$T = C_1 e^{a\theta} + C_2 e^{-a\theta} + b \qquad \text{(II-38)}$$

The constants may be determined by substituting the boundary conditions of equations (II-35) and the matching conditions of equations (II-36) into equation (II-38). The final solutions can be written in the form below.

$$\frac{T_1 - b_1}{b_2 - b_1} = \frac{1}{\xi} \frac{\cosh a_1 \theta}{\cosh a_1 (\pi - \alpha)} \quad \text{for } 0 \leq \theta \leq (\pi - \alpha) \qquad \text{(II-39a)}$$

$$\frac{T_2 - b_2}{b_2 - b_1} = \left(\frac{1}{\xi} - 1\right) \frac{\cosh a_2 (\pi - \theta)}{\cosh a_2 \alpha} \quad \text{for } (\pi - \alpha) \leq \theta \leq \pi \qquad \text{(II-39b)}$$

where

$$\xi = 1 + \frac{a_1}{a_2} \frac{\tanh a_1(\pi - \alpha)}{\tanh a_2 \alpha} \quad \text{(II-40a)}$$

$$a_i = \frac{h_i r^2}{K_s t} \quad \text{(II-40b)}$$

$$b_i = \left[\frac{1}{h_i} (q/A)_c + T_B \right] \quad \text{(II-40c)}$$

The subscripts refer to the section of the tube wall in which the quantities are evaluated. (1) refers to the boiling region and (2) refers to the vapor region.

F. Method of calculation.

The temperature distribution around the circumference of the tube is described by equations (II-39). These calculations may be carried out when the parameters in the equations are known. The necessary values can be determined from the equations developed in earlier sections of the analysis. There are two difficulties involved in making these calculations.

First; since the properties of the fluid depend on temperature, it is necessary to assume a temperature for the evaluation of properties before the calculations can be made. The temperature at the bottom of the tube was taken as representative of the temperature level of the vapor in the thin film. The properties were evaluated at the average film temperature. It was also necessary to assume a mean tube wall temperature in order to evaluate the radiation. This was easily done since the temperature distribution is fairly insensitive to small changes in the radiation.

Second; the conduction of heat in the tube wall presents a complication to the calculation of the boiling heat transfer coefficient. The local heat transfer per unit area in the boiling section was greater than the overall mean heat transfer rate. Thus it was necessary to assume a value of $(q/A)_T$ to use in equation (II-11).

The number of iterations required for each calculation was small because the analysis is fairly insensitive to the assumed values. A set of calculations were made which resulted in the preparation of a group of figures which gave tube temperature as a function of heat transfer rate, flow rate and position along the tube. Temperature profiles were derived from these figures for any given conditions.

The steps in the calculation procedure are:

1. Assume values for T_w , $\bar{T}_w$ and $(q/A)_T$.
2. Calculate X_M and find $\frac{\alpha}{\pi}$ from equation (II-21) or Figure 11.
3. Calculate h_{1b} from equation (II-11).
4. Calculate h_{1v} from equation (II-28).
5. Calculate a_1 , b_1 and ξ from equations (II-40).
6. Calculate T_1 from equations (II-39).
7. Check the assumed values of T_w , $\bar{T}_w$ and $(q/A)_T$.

The results of these calculations are discussed in Chapter IV. The temperature calculations are shown in Figures 12 to 22.

III EXPERIMENTAL PROGRAM

A. Introduction.

The general object of this investigation has been to examine the boiling of a liquid flowing through a tube when the tube wall temperature is much higher than the boiling temperature of the liquid. That is, when the boiling heat transfer takes place in the film boiling regime. It was proposed to determine first if it were possible to maintain stable film boiling on the inside of a heated, horizontal tube. It was next proposed to determine experimentally the relation between tube wall temperature, heat transfer rates, fluid flow rates and fluid properties over a range suitable for the evaluation of the analysis.

In order to prepare a fully instrumented and carefully controlled apparatus, two preliminary experiments were constructed. The object of these experiments was to determine whether or not stable film boiling occurs on the inside of tubes and to obtain some order of magnitude estimates of heat transfer coefficients to support the design of the final experiment.

The more important of these preliminary experiments was constructed to allow visual and photographic observation of the boiling process. The primary component of this apparatus was a glass tube coated with a semi-transparent, electrically conducting material. Tubes of this type are commercially available. The surface coating of the tube was used as a resistance heater to provide the required heat transfer. A system was built to pump a low boiling point liquid through the tube.

Visual and photographic observation of the operation of this apparatus confirmed the postulation that film boiling does occur on the inside of tubes in a stable state. A similar visual test section was incorporated in the later experiments and is described in more detail in Appendix C. The flow pattern which was observed, shown in Figure 7, was quite similar to that discussed by Bromley (ref. 5) for the film boiling on the outside of a horizontal rod. The inside diameter of the tube used in these tests was 0.418 inches.

The vapor film observed near the tube wall appeared to support the liquid. The vapor produced by the boiling flowed upward in the film under the action of bouyant forces and collected in a vapor layer at the top of the tube where it flowed downstream to the tube outlet. Thus the basic flow pattern observed was that of stratified flow.

The second preliminary experiment consisted of a tube which was heated by condensing steam. As Berenson (ref. 3) points out, better control of the film boiling process is obtained when the temperature difference is the controlled variable. In this way it is possible to obtain film boiling without passing through the complete nucleate boiling region. The inside diameter of the tube used in this experiment was 0.402 inches and the heated section was 24 inches long. Data obtained in these tests confirmed the observations in the visual experiments and provided useful information for the design of the more fully instrumented apparatus. Heat transfer coefficients calculated from these measurements were of the same order of magnitude as those calculated from Bromley's equation for film boiling on the outside of horizontal rods. (See equation II-1).

B. Description of the Apparatus.

A more detailed description of the apparatus is included in Appendix C but a brief discussion of the major components will be given here to provide continuity. The apparatus consisted of three primary sections. Schematic diagrams of these sections are shown in Figures 2, 3, and 4. They are: (1) the circulation system used to provide the flow of the test fluid and to control the state of the fluid throughout the system. (2) the visual test section similar in nature to that mentioned in the introduction composed primarily of an electrically conducting glass tube. (3) the quantitative test section used to obtain relatively accurate measurements of the tube wall temperature and heat transfer rates. Photographs of a part of the apparatus are shown in Figures 5 and 6.

The circulation system included a pump to maintain the flow and two hot water preheaters to control the temperature of the fluid at the test section inlet. A cold water condenser was used to recondense the vapor formed by the boiling in the heated tube. Two rotameters were provided to measure the fluid flow rate. The rotameters were of different capacity and connected in parallel to allow more accurate flow measurements.

Thermocouples were inserted into the flow just before the test section inlet and at the condenser outlet to allow proper control of the fluid temperature. A pressure gage was connected to the system to measure the pressure level at the inlet of the test section.

The visual test section was composed of a 13mm. glass tube coated with a semitransparent, electrically conducting material which was used as a resistance heater. Power was supplied to the glass tube through a variable transformer. This allowed a variation in the heat transfer rate to be made. An ammeter was installed to read the current passing through the coating on the tube. The heated section of the tube was nine inches long and had an inside diameter of 0.418 inch.

The quantitative test section was constructed around a stainless steel tube 15 inches long. The inside diameter of the tube was 0.402 inch. A d.c. power source with a high current capacity was connected to the ends of the tube and the tube was used as a resistance heater. A set of six guard heaters were wrapped around the test tube at a diameter of 2.5 inches. The guard heaters were made of nichrome heater wire and were individually controlled with variable transformers. The space between the test tube and the guard heaters was filled with an insulating material of known thermal conductivity. Thermocouples were located on the test tube at six positions. Directly below this line of thermocouples was another set of thermocouples just inside the guard heater ring.

Matching of the temperatures read on corresponding pairs of the thermocouples insured close control of the radial heat transfer out of the test section. The entire test section was insulated further especially to reduce end losses. Guard heaters were located on the power leads to prevent heat losses by conduction in the cables.

The test fluid in all the experiments was distilled Freon - 113. Its low boiling point and low latent heat made it particularly suitable for these tests.

C. Measurements and Accuracy.

Temperatures were measured at the surface of the heated tube, near the guard heaters and at two points in the liquid flow. All temperatures were measured with carefully constructed chromel-alumel thermocouples. The temperature of the fluid just ahead of the test section inlet was recorded by inserting a thermocouple in the flow. The temperature of the liquid was also measured in the same way at the outlet of the condenser. This measurement was taken to insure complete recondensation of the vapor produced in the heated tube.

The temperatures near the guard heaters were recorded by thermocouples set $\frac{1}{8}''$ inside the guard heater ring. The thermocouples were set inside of ceramic tubing and separated from the guard heater wires and the guard heater frame. The hot junctions of these thermocouples were imbedded in the insulation between the test tube and the guard heater frame.

The temperature of the tube wall was measured by thermocouples tied to the tube. A thin (0.002 inch) piece of mica was used to separate the hot junctions from the metal surface to avoid any stray electrical contact. Calculations were made to determine the temperature difference between the inner and outer surfaces of the tube caused by the uniform generation of heat in the volume of the tube wall. Because of the low heat flux in the experiments this difference was a maximum of 3° F.

The temperatures at the bottom of the tube were the ones recorded in the majority of the tests. These temperatures were used to compare with corresponding temperatures under the guard heaters.

The heat transfer rate was determined by measuring the current in the tube wall and calculating the resistivity of the metal based on the temperature at the bottom of the tube. The power input per unit surface area of the tube was calculated from the following relation:

$$(q/A_s) = \frac{1}{A_s}\left(\rho' \frac{L}{A_c}\right) I^2 \tag{III-1}$$

A_s represents the surface area based on the inside diameter, ρ' the resistivity of the metal which is a function of temperature, L the length of the element, A_c the cross sectional area of the tube wall and I the current in the tube wall.

The current was measured by recording the voltage drop across a shunt in the power line leading from the generators. The resistance of the shunt had been calibrated at the National Bureau of Standards to within 0.1% under testing conditions. Under the conditions of operation in the laboratory the error in the measured value of the current should not be excessive.

The resistivity of the tubing was evaluated as a function of temperature based on values obtained from a standard materials handbook.

A resistance bridge was designed to provide a check on the power input found by using equation (III-1). Although the readings were actually the voltage drop across the test tube plus a portion of the power leads, close agreement was found between the values from equation (III-1) and the relation $P = I\,E$, where E represents the measured voltage drop.

Close control of radial heat losses was provided by the guard heater arrangement. A heat loss of 1% of the power input required about 100° F temperature difference between the tube temperature and the temperature near the guard heater ring. In actual testing the temperature differences allowed were considerably less than 100° F.

Guard heaters were placed on the electrical leads in order to prevent significant end losses by conduction down the cables. The significant source of end losses was inherent in the design and little could be done to reduce these losses in the apparatus. The heated tube was connected to the inlet and outlet tubes with flanged joints separated by a Teflon gasket $\frac{1}{8}$ " thick. Since the inlet and outlet tubes were not in the heated section the temperatures of the tubes were low. Thus a large temperature gradient existed in the gasket which allowed considerable axial heat transfer at the end of the tube. It appears, then, that the heat transfer rate was controlled to within, perhaps, 2% except near the ends of the heated section where axial heat conduction caused large end losses.

The flow rates were measured with a rotameter. The rotameters were calibrated with a measurement of the total weight of liquid pumped through them over a measured time interval. The maximum error in the scale readings was 5% in the range used in the experiments. Much larger errors were found when the flow rate was a small fraction of the capacity of the rotameter.

D. <u>Experimental Technique</u>.

A certain amount of difficutly was encountered in attempting to operate the equipment. It was thought wise to avoid temperatures greater than 1000° F to prevent damage to the apparatus. Since the heat input was the controlled variable it would have been necessary to pass completely through the nucleate boiling regime to the burnout point if film boiling were to be obtained by a gradual increase in power input.

It was found that film boiling in the tube could be started directly without the danger of abrupt temperature increases by another method.

With no liquid flow, the test section was heated with the guard heaters and the main power supply until a temperature greater than that required to produce film boiling (about 500° F in these tests) was reached by all parts of the test section. When this temperature level was reached the fluid was circulated through a secondary loop formed by the visual test section and the circulation system. The preheater hot water supply was adjusted at this point to give approximately the fluid conditions required in the test.

The main power supply was then turned on and adjusted to the approximate level required to maintain film boiling. Without delay the fluid was pumped through the heated section of the tube. The change from the loop including the visual test section to the loop including the quantitative test section was accomplished by a set of quick opening valves which were operated by hand. Haste was not required in this operation but much delay in starting the fluid through the heated tube could have resulted in overheating the tube.

The desired settings of the power input, flow rate and guard heater temperatures were adjusted after the boiling process was started.

When the temperature of the test section or the power input was too low when the flow was started, continuous operation in the film boiling region was not possible. The tube temperature near the inlet end would start falling and eventually reach a level equivalent to that in nucleate boiling. The cool section of the tube would slowly grow until the entire tube was in the nucleate boiling regime.

It was observed in the visual test section that there was an interface between the film boiling section and the nucleate boiling section which would gradually move downstream. This interface was also observed near the outlet end of the heated section. In this case the interface would move gradually upstream until the entire tube was in the nucleate boiling regime.

The warm up and starting procedure for the visual test section was the same as that for the quantitative test section. Since no temperature measurements were made in the visual tests, the time to start the flow was determined in a slightly different manner. The tube was filled with liquid and the flow passed through a secondary loop. The valve at the outlet of the tube was kept open. When the power supply was turned on the fluid remaining in the tube would begin to boil. Shortly after the tube had boiled dry the flow was started. This method of starting the film boiling in the visual tests proved quite satisfactory.

After the boiling was started in the quantitative test section, the values of the temperatures, flow rate and power input were recorded at short intervals of time. Adjustments in the power supplied to the guard heaters were made as required. When the temperatures on the tube and near the guard heaters were properly matched and reached steady values, equilibrium was considered to have been reached and the data were recorded.

The voltage output of the thermocouples was measured with a potentiometer. The voltage drop across the shunt in the power line and across the measuring points of the resistance bridge for determining the voltage drop across the test section were also measured with the potentiometer. Flow rates were read from the rotameter scale.

E. Data Recorded.

Temperatures at the bottom of the tube were measured at the following points: x = 0.083 ft., x = 0.271 ft., x = 0.5 ft., x = 0.75 ft., x = 0.978 ft., and x = 1.17 ft. Because of the large end losses the temperature nearest the outlet end of the tube has little value in discussing the analysis. For this reason the comparison of predicted temperature to experimental temperature in the following section of the report was made for only the first 12 inches of the test section.

Experiments were run with the velocity of the liquid at the test section inlet at three values. These were: V_o = 1.23 ft./sec., V_o = 1.85 ft./sec. and V_o = 2.46 ft./sec.

The range of mean heat transfer rate per unit area was from 10,000 Btu/hr ft.^{2} to 18,600 Btu/ hr ft.^{2}.

Two tests were made where the total length of the test section was 24 inches.

Three tests were made with the 15 inch test section when it had been rotated on its axis by 180°. In this way values of the temperature at the top of the tube were measured. These tests were run with, as near as possible, the same heat transfer rate and flow rate as in three previous tests where the temperatures at the bottom of the tube were recorded.

The fluid used as the test fluid in all experiments was Freon - 113 which boils at 125° F at the pressures in the tests. The liquid state at the test section entrance was near saturation. A small amount of subcooling was required in order to prevent local boiling in the heat exchanger and cavitation in the tubing and valves between the preheater and the test section. Fluid temperatures were recorded for each test.

IV RESULTS AND CONCLUSIONS

A. Discussion.

The results of the calculations from the analysis and the experimental data are shown in Figures 12 to 22. Figures 12 to 17 show the comparison of theoretical and experimental temperature differences as functions of the distance from the inlet end of the tube. Each curve represents a specific heat transfer rate and fluid flow rate. The data shown in these figures are for the first 12 inches of the heated tube. End losses affect the temperature in the 3 inches of the tube near the outlet to a considerable degree and only serve to confuse the comparison. All temperature differences in these figures are the difference between the temperature of the tube wall at the bottom of the tube and the saturation temperature of the liquid. The only exception is Figure 18 where temperatures at the top of the tube are reported.

Figure 19 shows the experimental temperature difference as a function of distance from the tube inlet for two different test section lengths. The first test section was 24 inches long. The second was 15 inches long. This comparison serves to illustrate the effect of the end losses on the measured temperature difference at the bottom of the tube.

The temperature difference at the top of the tube and the temperature difference at the bottom of the tube for a single fluid flow rate and heat transfer rate are shown in

Figure 18. Both theoretical and experimental values are plotted.

Figures 20 and 21 show the heat transfer rate as a function of the theoretical temperature difference for three flow rates at a specified distance from the inlet end of the tube. Experimental values at corresponding flow rates and position are also shown in these figures.

It was found that the analysis predicted a variation of the temperature difference at the bottom of the tube with flow rate to the one-tenth power. If the reduced temperature difference is defined as

$$\Delta T_{RED} = \left\{ \frac{V_0}{(V_0)_1} \right\}^{0.1} \left(T_{WALL} - T_{SAT} \right) \qquad \text{(IV-1)}$$

the theoretical reduced temperature difference at any location on the tube, x_1 , can be plotted as a function of heat transfer rate with a single curve. Figure 22 shows such a curve for $X/L = 0.5$. The experimental data are also compared to the theory in this figure.

It can be seen from the figures that the temperature level of the tube wall has been predicted fairly well as a function of heat transfer rate. The temperature differences calculated from the analysis, in general, rise rapidly near the inlet end of the tube to a relatively steady value. A gradual decrease in the temperature difference is predicted as the value of X/L increases from 0.25 to 1.0. The maximum value of this decrease calculated was 5% of the temperature difference. On the other hand, the experimental values of the temperature difference increase rapidly near the inlet end of the tube but continue to increase gradually with an increase in X/L for most cases. A decrease in the temperature difference with increasing X/L was observed in two tests with high flow rates and heat transfer rates.

It is possible to estimate the size of some of the errors caused by the assumptions in the analysis and to partially account for this discrepancy.

It should first be noted that the effects of end losses, shown in Figure 19, are significant for about the last 3 inches of the test section. Since the major source of end losses in the experiments was conduction of heat to the inlet and outlet tubes, it is reasonable to estimate the end losses at the inlet end on the basis of this figure. The flow in the inlet tube was entirely liquid and the flow in the outlet tube was a two phase mixture of liquid and vapor. Thus it seems possible that the end losses at the inlet end might be somewhat greater than those at the outlet end. In any case, it was to be expected that the measured temperature differences near the inlet end of the heated tube would be less than those calculated from the theory where axial heat conduction was omitted.

Three approximations in the analysis caused small errors in the calculation of the temperature difference. It was found that these errors, although small, were all in the direction of underestimating the tube temperature and that the errors increased in magnitude as X/L increased. Thus the combination of the three small errors might serve to partially explain the discrepancy in the temperature variation with tube length.

The first of these approximations was that the effect of vapor friction at the top of the tube had a negligible effect on the area ratio calculations. An approximate, perturbation analysis was carried out to check the magnitude of the errors caused by this assumption. It was found that the maximum error in the calculated temperature difference was of the order of 1% to 2% at X/L = 1.0. The approximation improved for positions nearer the inlet end of the tube. This error was always in the same direction. Neglecting the frictional effects caused the calculated temperature differences to be lower than those found in the perturbation analysis. If friction in the vapor layer were considered, the velocity of the vapor would be slightly reduced, the cross sectional area of the flow of vapor would be slightly increased and the heat transfer coefficient to the vapor would also decrease. The combination of these effects would result in higher calculated tube wall temperatures since the heat transfer coefficient for the vapor layer was less than the heat transfer coefficient for the boiling liquid.

The second approximation which could cause a small error in the calculated temperature difference at the bottom of the tube was the approximation of using the mean boiling heat transfer coefficient in the conduction analysis. The boiling heat transfer coefficient was actually a function of the angle from the bottom of the tube. Since the variation was small, the averaging factor γ was used to approximate the mean heat transfer coefficient. The local heat transfer coefficient at the bottom of the tube was always given by equation (II-9) with a unit value given to the angle factor. In the calculations, the multiplier used was the factor which varied with tube length. The error in the heat transfer coefficient at the bottom of the tube varied by about 2% as X/L increased from 0.25 to 1.0. The average value of the boiling heat transfer coefficient was correct at all positions but the local value at the bottom of the tube was not exact. This error was always in the direction of underestimating the temperature rise with tube length at the bottom of the tube.

The third approximation which could cause the temperature rise with tube length to be underestimated slightly was the evaluation of the heat transfer by radiation. The view factor from the tube wall in the vapor region to the liquid should actually be a function of the area ratio. The calculations were carried out with a unit view factor at all points on the tube surface. It is difficult to estimate the magnitude of the error in the temperature at the bottom of the tube. It can only be stated that the error should always be in the direction of underestimating the temperature difference at the bottom of the tube and that the size of the error sould increase as the angle α increases. Since the heat transfer by radiation was always a small part of the total heat transfer, these errors would be small. Very rough, approximate calculations indicate that the error in the rise of calculated temperature difference at the bottom of the tube might be of the order of 1%.

The errors that have been discussed in the previous paragraphs are all small in absolute magnitude and are well within the possible errors from other sources, such as the estimation of the heat transfer coefficient for the vapor layer. The discussion has been included to show the possibility of an explanation for the discrepancy in the calculated temperature distribution with X/L, not to explain errors in the level of the calculated temperature difference.

A check was made of the percentage rise in temperature difference from the bottom of the tube to the top of the tube. This comparison for one of the three tests run is shown in Figure 18. The comparison of percent change in temperature difference at the two positions on the circumference appears to be quite good. The other two tests showed similar results. The experimental temperature differences shown in this figure were not obtained at the same time. The experiment was operated with the thermocouples at the bottom of the tube and the data recorded. The test section was then rotated on its axis 180° and operated a second time with the thermocouples at the top of the tube. The fluid flow rate and heat input were carefully matched to those measured in the previous test. Thus small errors might have been caused by not obtaining this data all at the same time.

The variation of calculated temperature difference at the bottom of the tube with fluid flow rate shown in Figures 20 to 22 does not seem quite as great as that measured in the experiments. A possible explanation of this difference may be found in the velocity profile coefficient for the vapor film. It is possible that the effective frictional drag in the tangential direction on the vapor in the thin film is a function of the flow rate in the tube. Such a variation could account for the differences seen in the figures if the drag force decreased with increasing flow rate. The difference may, of course, be caused by some other error which has not been accounted for.

B. Summary of Conclusions.

1. Stable film boiling occurs on the inside of horizontal tubes in forced convection over a range of operating conditions.
2. An idealized flow model has been developed which appears to represent the flow to a reasonable degree of accuracy.
3. Photographs and visual observation of the boiling in a glass tube support the assumptions made in the idealized flow model.
4. The flow of a liquid in film boiling on the inside

of a tube is, in the region investigated, primarily stratified flow where a thin vapor film separates the liquid from the tube wall in the lower portion f the tube.

5. A method of calculation has been developed which allows the temperature difference between the tube wall and the boiling fluid to be calculated as a function of the heat transfer rate, the fluid flow rate and the fluid properties with an accuracy of ± 15%.

6. The assumptions are valid only in the region where the mass flow of vapor is small compared to the total mass flow.

7. The region in which the assumption of stratified flow is valid has not been determined except that the accelerating flow in the film boiling process seems to encourage the formation and preservation of a stratified flow.

NOMENCLATURE

English Symbols

A = Area

a_1, b_1 = Non-dimensional parameters defined in equation (II-40)

b = Thickness of the vapor film

C = Constant

C_p = Specific heat at constant pressure

D = Diameter

De = Equivalent diameter

E = Potential difference

f = Friction factor

g = Acceleration of gravity

h = Heat transfer coefficient

I = Electric current

K = Thermal conductivity

K_s = Thermal conductivity of the steel tube

L = Length of the tube

P = Pressure

q = Heat transfer rate

(q/A) = Heat transfer rate per unit area

$\overline{(q/A)}$ = Mean heat transfer rate per unit area

r = Radius

T = Temperature

t = Thickness of the tube wall

V = Velocity

V_o = Velocity of the liquid at the test section inlet

W = Mass flow rate

x = Distance from the tube inlet

Xm = Non-dimensional tube length-flow rate factor defined in equation (II-22)

y = Distance from the tube wall in the vapor film

Greek Symbols

α = Interface angle shown in Figure 7

β' = Experimentally determined coefficient in the expression for the boiling heat transfer coefficient

γ = Averaging factor for the local boiling heat transfer coefficient $\gamma = \frac{1}{(\pi-\alpha)} \int_0^{(\pi-\alpha)} \left\{ \frac{\sin\theta}{\theta} \right\}^{1/3} d\theta$

ϵ_s = Emissivity of the tube surface

θ = Angle from the bottom of the tube shown in Figure 7

λ = Latent heat of the liquid

λ' = Average heat content of the vapor (see discussion in Appendix B)

μ = viscosity

ξ = Non-dimensional number defined in equation (II-40)

ρ = Density

ρ' = Electrical resistivity

σ = Stefan-Boltsman constant

Subscripts

B = Boiling temperature

b = Bulk temperature

c = Convection

co = Convection in the absence of radiation

i = Horizontal liquid-vapor interface

L = Local conditions

LB = Local conditions in the boiling region

LV = Local conditions in the vapor region

r = Radial

RAD = Radiation

S = Refers to surface area

T = Total

V = Vapor

W = Conditions at the tube wall

1 = Evaluated in the region $0 \leq \theta \leq (\pi - \alpha)$

2 = Evaluated in the region $(\pi - \alpha) \leq \theta \leq \pi$

BIBLIOGRAPHY

1. Rohsenow, W. M., Heat Transfer - A Symposium, University of Michigan, 1952, pp. 101
2. Westwater, J. W., "Boiling of Liquids", Advances in Chemical Engineering, Academic Press, Inc., New York, 1956
3. Berenson, P.J., "Transition Boiling Heat Transfer from a Horizontal Surface", M.I.T. Division of Sponsored Research Technical Report No. 17, 1960
4. Ellion, M. E., "A Study of the Mechanism of Boiling Heat Transfer", Memorandum No. 20-88, Jet Prop. Lab., California Institute of Technology, 1954
5. Bromley, L. A., "Heat Transfer in Stable Film Boiling", United States Atomic Energy Commission, AECD-2295, 19-
6. Bromley, L. A., LeRoy, N. R. and Robbers, J. A., "Heat Transfer in Forced Convection Film Boiling", Industrial and Engineering Chemistry, vol. 45, 1954, pp. 2639
7. Hsu, Y. Y., and Westwater, J.W., "Film Boiling from Vertical Tubes", Presented at the A.S.M.E.-A.I.Ch.E. Joint Heat Transfer Conference, 1957
8. Hsu, Y. Y. and Westwater, "Approximate Theory for Film Boiling on Vertical Surfaces", Presented at the Third National Heat Transfer Conference, A.S.M.E.-A.I.Ch.E., 1959
9. Bradfield, W. S., "Plane Laminar Forced Convection Film Boiling with Subcooling", Convair Scientific Research Laboratory Research Note 35, 1960

10. Cess, R. D. and Sparrow, E. M., "Film Boiling in a Forced Convection Boundary Layer Flow", A.S.M.E. Paper No. 60-WA-148, 1960

11. Graham, R. W., Hendricks, R. C., Hsu, Y. Y. and Friedman, R., "Experimental Heat Transfer and Pressure Drop of Film Boiling Liquid Hydrogen Flowing through a Heated Tube", Presented at the 1960 Cryogenic Engineering Conference.

12. von Glahn, V. H. and Lewis, J. P., "Nucleate and Film Boiling Studies with Liquid Hydrogen", Advances in Cryogenic Engineering, vol. 5, 1960

13. Sterman, L. S. and Styshen, N. G., Zh. Tekh. Fiz., U.S.S.R., vol. 22, No. 3, 1952, pp. 446

14. Bromley, L. A., Brodkey, R. S. and Fishman, Norman, "Heat Transfer in Condensation, Part II, Effect of Heat Capacity on Condensate", Industrial and Engineering Chemistry, vol. 44, 1952, pp. 2966

15. McAdams, W. H., Heat Transmission, 3rd Edition, McGraw-Hill Book Co., Inc., New York, 1954

16. Jacob, M., Heat Transfer, vol. 1, John Wiley & Sons, New York, 1955

17. Moody, L. F., "Friction Factors for Pipe Flow", Trans. Am. Soc. Mech. Engrs., vol. 66, 1944

APPENDIX A

DETERMINATION OF THE COEFFICIENT β'

The value of the constant β' in equation (II-11) is determined by the velocity profile in the vapor film. If the flow of vapor in the tangential direction is laminar and the liquid at the liquid-vapor interface exerts no drag on the vapor, the variation of vapor velocity with distance from the tube wall may be written in the following form.

$$V_v = C\left(by - \frac{y^2}{2}\right) \tag{A-1}$$

where b is the film thickness and y is the distance from the tube wall. The constant can be determined in terms of the vapor flow rate by a simple integration.

$$C = \frac{3\omega_v}{\rho_v b^3} \tag{A-2}$$

Then the value of $(Tw)_T$ can be found from the slope of the velocity profile at the wall.

$$(\tau_w)_T = -\mu_v \frac{\partial V_v}{\partial y}\bigg|_{y=0} = -3\frac{\mu_v w_v}{\rho_v b^2} \tag{A-3}$$

Similarly, if the liquid-vapor interface is assumed to be completely rigid the velocity in the film may be written as

$$V_v = C(by - y^2) \tag{A-4}$$

and the wall shearing stress calculated as

$$(\tau_w)_T = -12 \frac{\mu_v \omega_v}{\rho_v b^2}$$

since there is a drag force on both sides of the vapor.

This derivation is perhaps unnecessary since the relations are well known but has been included for clarity.

If the flow in the vapor film is laminar and the tangential velocity profile is parabolic in form, limits can then be set on the magnitude of the friction drag. That is,

$$\frac{3\mu_v \omega_v}{\rho_v b^2} \leq \left| (\tau_w)_T \right| \leq \frac{12\mu_v \omega_v}{\rho_v b^2} \qquad \text{(A-5)}$$

The value of the constant multiplier in this equation can then be determined as the value which best fits experimental data. This was done by Bromley (ref. 5) for natural convection film boiling on the outside of a tube. The value of the constant in equation (II-1) that he determined was 0.62. The best fit to the data in this investigation was for a value of this constant of 0.65.

APPENDIX B

EVALUATION OF PROPERTIES

The fluid properties which appear in the non-dimensional groups in the analysis are, in general, functions of temperature. Bromley (ref. 14) discussed the method of evaluating these properties. He suggested that, in the interest of simplicity, all properties except the heat content of the vapor can be evaluated at the average film temperature without significant error.

In a paper considering film condensation Bromley (ref. 14) derives an expression for the effective heat content of the film. His derivation considered the velocity profile and local heat conduction and results in the expression

$$\lambda' = \lambda\left\{1 + \frac{0.4\, c_p \Delta T}{\lambda}\right\}^2 \qquad \text{(A-6)}$$

The velocity profile used in this derivation was the one which results from the assumption, in film boiling, that the liquid exerts no drag on the vapor. This is quite reasonable in the condensation process where the film is composed of liquid, but not exactly the case for film boiling as was shown in Appendix A. The effective film temperature for estimating the heat content of the vapor should be between the arithmetic mean temperature and the effective temperature in equation (A-6). It does not seem that the analogy between film condensation and film boiling is exact in this case as Bromley suggested.

Since the values of $\frac{C_p \Delta T}{\lambda}$ encountered in this investigation were always less than unity, the difference between evaluating the heat content of the vapor at the mean film temperature and using equation (A-6) caused small errors in the calculation of the heat transfer coefficient. The maximum difference was 10%. The true value of the heat content of the vapor should be between the two values, indicating that the maximum error should be, at least, less than 10%. The calculations in this report were based on the evaluation of the heat content of the vapor at the arithmetic mean temperature of the film. A better estimate of the value of the heat content of the vapor would be required for values of $\frac{C_p \Delta T}{\lambda}$ much in excess of unity.

The properties of Freon - 113 vapor were evaluated as functions of temperature on the basis of data furnished by the manufacturer. The temperature range of this data was insufficient to evaluate the properties at some of the higher temperatures in these tests. The values of the properties in this region were obtained by extrapolation of the property - temperature relations at lower temperatures.

APPENDIX C

EXPERIMENTAL DESIGN

The apparatus may conveniently be divided into three sections for the purpose of discussion. These sections are: (1) The circulation system which was used to control the fluid flow rate and temperature; (2) The visual test section which was used to obtain visual and photographic evidence of the flow pattern; (3) The quantitative test section which was used to obtain measurements of the heat transfer rate and tube wall temperatures. These three sections are shown schematically in Figures 2, 3 and 4. Photographs of the major portion of the apparatus are shown in Figures 5 and 6.

(1) The Circulation System.

The major parts of the circulation system were the pump and motor, the rotameters, the preheaters, the pressure gage, the condensor, the liquid reservoir, and the fluid temperature thermocouples.

The Pump and Motor: The pump used in this apparatus was a Vanton Pump, model XB-S90 with a neoprene "flex-i-liner". The pump was connected to a 1 HP electric motor. The pump design was such that there were no rotating seals which might allow impurities to dissolve in the test liquid.

The Rotameters: Two Brooks Rotameters were installed in parallel in the system. The smaller meter had a maximum capacity of 1.6 gallons per minute of Freon - 113. The larger meter had a maximum capacity of 6.0 G.P.M. of Freon - 113. The measured flow rates of the rotameters were calibrated to ± 5% when readings on the lower third of the scales were avoided.

<u>The Preheaters</u>: The first preheater constructed was a 6 inch diameter coil of 1/2 inch O.D. copper tubing submerged in a flow of hot water. The total length of the tubing was 20 ft. The coil was enclosed by an annulus of sheet brass to contain the water flow. It was found that, if heater water temperatures were high enough to provide a satisfactory temperature rise in the Freon, local boiling occured in the preheater. For this reason a second preheater was placed in series with the first. The additional heat transfer surface allowed the same temperature rise to be obtained with lower heating water temperatures.

The second preheater was constructed of 40 copper tubes, 1 foot long and 1/4 inch O.D. These were used as a double pass heat exchanger. The heater water flow was contained in a brass casing around the tubes.

<u>The Pressure Gage</u>: The pressure gage was a standard 0 to 100 psi. gage which had recently been calibrated. In the tests reported here the pressure levels were low so that the pressure measurements were of little consequence.

<u>The Condenser</u>: The condenser was constructed of a 20 foot length of 1/2 inch O.D. copper tubing wrapped in a

6 inch diameter coil. The coil was cooled by a flow of cold water. The condenser coil was enclosed in an annulus of sheet brass to contain the cooling water.

The Liquid Reservoir: The liquid supply was stored in a cylindrical brass reservoir with a capacity of about 1.5 gallons. A pressure relief valve was attached to the reservoir to bleed off any Freon vapor not recondensed in the condenser and maintain the system pressure. In practice, the relief valve was never in operation since the condenser was overdesigned to assure complete recondensation of the vapor.

The Fluid Temperature Thermocouples: Chromel-alumel thermocouples were placed in the fluid flow just before the test section inlet and at the condenser exit. The thermocouple wires were enclosed in a small stainless steel tube which allowed the measuring junction to be set nearly at the center of the tube. A compression fitting with a Teflon sealing gasket was used to prevent leakage at the thermocouples. The thermocouples were made from B.&S. gage no. 28 glass and enamel insulated, duplex, cromel-alumel wire.

(2) The Visual Test Section.

The major component of the visual test section was a glass tube 48 inches long which was coated with an electrically conducting, semitransparent material. The inside diameter of the tube was 0.418 inches. Copper clamps were attached to the tube to make electrical connections. The heated section of the tube was 9 inches long and located near the center of the 48 inch length so that the flow could be observed both before and after the heated section.

Power was supplied through a variable transformer connected to a 220 volt a.c. power line. An ammeter was installed in the power lead to measure the current flow.

The glass tube was attached to the circulation system by 1/2 inch copper tubing compression fittings in which the compression sleeve had been replaced by a Teflon gasket. Quick opening valves were placed in the line at either end of the glass tubing to allow the flow to bypass the visual test section when the quantitative tests were being carried out.

A 48mm. glass tube was placed around the conducting glass tubing to protect the tube from possible breakage and to isolate the uninsulated 220 volt circuit.

(3) <u>The Quantitative Test Section</u>.

The quantitative test section was composed of a heated tube and system for reducing the losses from the heated tube. Thermocouples were provided to measure the temperature of the tube at several locations.

The heated tube was a type 304 stainless steel tube, 15 inches long, with an inside diameter of 0.402 inches and an outside diameter of 0.500 inches. The tube was heated by passing an electric current through the tube wall. The power supply was a generator set which was available in the laboratory.

Chomel-alumel thermocouples were tied to the tube over thin (0.002 inches) pieces of mica in a line at the bottom of the tube. Thermocouples were placed at the following distances from the inlet end of the tube: x = 1"; x = 3 1/4"; x = 6"; x = 9"; x = 11 3/4"; x = 14".

The ends of the tube were flanged. The electrical input was supplied through the bolts that held the flanges to the flanges on the inlet and outlet tubes.

A guard heater was wrapped on a 2.5 inch diameter frame which surrounded the heated tube. The guard heater was constructed in six, individually controlled sections. The heaters were made from 28 gage nichrome heater wire wrapped at 10 turns per linear inch of the frame. The frame used to support the guard heaters was a 2.5 inch diameter aluminum tube. The heater wire was separated from the frame by glass sleeving which had been slipped over the wire. Power was supplied to the guard heaters through six small variable transformers which were connected to a 110 volt a.c. power line.

Thermocouples were placed with the measuring junctions 1/8 inch inside the guard heater ring. These thermocouples were placed so that each thermocouple on the guard heater frame corresponded to one of the thermocouples on the tube. That is, each pair of thermocouples was placed on the same radius. The thermocouples on the guard heater frame were set in ceramic tubing to separate the thermocouple wire from the heater wire and the guard heater frame.

The volume between the heated tube and the guard heater frame was filled with a carved piece of Uniblock insulation. The thermal conductivity of this material had recently been determined as a function of temperature in the laboratory. The entire test section assembly was encased in a layer of the same insulating material. Further insulation on the outside of the guard heaters allowed the capacity of the guard heaters to be reduced.

Guard heaters were wrapped around the power supply cables to control the effect of conduction down the cables. These guard heaters were made of 20 ft. of 28 gage nichrome heater wire. Thermocouples were tied to the power cables between the guard heaters and the heated tube to allow proper control of these heaters.

The ends of the heated tube were connected to the inlet and outlet tubes by flanges. The flanges were separated by a 1/8 inch thick Teflon gasket. The inlet tube was 15 inches long and the outlet tube was 6 inches long. These tubes were connected to the circulation system with quick opening valves. The valves allowed the quantitative test section to be bypassed in the visual tests.

Control of the power supply was provided by a control panel associated with the generator set. Thermocouple outputs were measured with a potentiometer.

Two of the tests were made with a quantitative test section of similar design which had a total length of 24 inches.

This test section was constructed with the flanges at the ends of the heated tube silver soldered to the tube. These joints failed after being heated to high temperature levels. The flanges in the 15 inch test section were welded to the heated tube.

Table I

THERMOCOUPLE LOCATIONS

The subscripts in the following tables indicate the location of the temperature measurements in the following manner.

A. $\underline{w}$ refers to the temperature of the tube wall.

B. $\underline{g}$ refers to the temperature on the guard heater ring.

C. inlet and outlet refer to the temperatures measured on the power supply cables between the guard heaters and the test section.

D. $\underline{f}$ refers to the temperature of the fluid just upstream from the test section.

E. The numerical subscripts give the position along the tube as shown below.

Runs 2 and 3

For the 24 inch test section

Subscript	X - ft.
1	0.083
2	0.333
3	0.75
4	1.25
5	1.67
6	1.92

Runs 4 to 25

For the 15 inch test section

Subscript	X - ft.
1	0.083
2	0.27
3	0.50
4	0.75
5	0.98
6	1.17

Table II

DATA FOR THE 24 INCH TEST SECTION

Temperatures at $\theta = 0$

Run No.	2	3
V_o - ft./sec.	1.23	2.46
I - amps.	244	271
E - volts.	3.33	3.70
(q/A)- Btu./hr.ft.^{2}	13000	16050
T_f - ^oF	108	100
T_{w1} - ^oF	639	643
T_{w2} - ^oF	730	750
T_{w3} - ^oF	750	739
T_{w4} - ^oF	741	744
T_{w5} - ^oF	720	754
T_{w6} - ^oF	660	694
T_{g1} - ^oF	694	701
T_{g2} - ^oF	704	714
T_{g3} - ^oF	710	725
T_{g4} - ^oF	711	729
T_{g5} - ^oF	730	740
T_{g6} - ^oF	723	726
T_{inlet}- ^oF	626	632
T_{outlet}- ^oF	522	510

Table III

DATA FOR THE 15 INCH TEST SECTION

Temperatures at $\theta = 0$

Run No.	4	5	6	7	8	9
V_o - ft./sec.	1.23	1.23	1.23	1.23	2.46	1.23
I - amps.	219	234	234	254	267	270
E - volts	1.75	1.93	1.93	2.11	2.23	2.30
(q/A)- $\frac{\text{Btu.}}{\text{hr.ft.}^2}$	10100	11800	11800	14300	15600	16500
T_f - ^oF	109	109	106	109	102	109
T_{w1} - ^oF	542	593	597	658	632	724
T_{w2} - ^oF	617	673	685	748	716	824
T_{w3} - ^oF	640	696	705	773	733	843
T_{w4} - ^oF	656	711	724	790	763	853
T_{w5} - ^oF	658	713	728	792	765	841
T_{w6} - ^oF	567	633	652	705	671	744
T_{g1} - ^oF	633	681	688	681	690	739
T_{g2} - ^oF	637	694	711	718	727	790
T_{g3} - ^oF	639	715	743	760	756	822
T_{g4} - ^oF	640	735	765	771	777	841
T_{g5} - ^oF	628	722	756	760	765	840
T_{g6} - ^oF	632	728	760	763	763	807
T_{inlet}- ^oF	630	634	634	653	669	702
T_{outlet}- ^oF	540	666	711	743	740	758

Table III (continued)

DATA FOR THE 15 INCH TEST SECTION

Temperatures at $\theta = 0$

Run No.	10	11	12	13	14	15
V_o - ft./sec.	1.85	2.46	1.85	2.46	1.85	2.46
I - amps.	282	288	233	238	242	260
E - volts	2.40	2.43	1.92	1.98	2.19	2.34
(q/A)- $\frac{\text{Btu.}}{\text{hr.ft.}^2}$	17900	18650	11400	11700	12500	14500
T_f - °F	109	102	109	103	106	102
T_{w1} - °F	728	729	535	509	601	621
T_{w2} - °F	807	803	613	532	660	665
T_{w3} - °F	828	818	638	601	665	666
T_{w4} - °F	841	813	653	626	682	697
T_{w5} - °F	838	809	655	628	689	699
T_{w6} - °F	741	729	516	535	630	617
T_{g1} - °F	773	765	628	530	662	646
T_{g2} - °F	818	805	643	592	626	653
T_{g3} - °F	837	818	644	599	680	656
T_{g4} - °F	841	818	665	614	695	676
T_{g5} - °F	811	783	655	606	686	668
T_{g6} - °F	800	777	656	600	683	662
T_{inlet} - °F	722	738	584	590	689	697
T_{outlet} - °F	769	769	607	598	670	620

Table III (continued)

DATA FOR THE 15 INCH TEST SECTION

Temperatures at $\theta = 0$

Run No.	16	17	18	19	20	21	22
V_o - ft./sec.	1.85	1.23	1.23	1.85	2.46	2.46	1.85
I - amps.	258	228	226	250	258	278	264
E - volts	2.37	1.90	1.83	2.07	2.13	2.36	2.24
(q/A)- $\frac{\text{Btu.}}{\text{hr.ft.}^2}$	14600	11000	10800	13400	14250	17100	15400
T_f - °F	108	108	108	102	103	105	105
T_{w1} - °F	661	553	540	588	579	670	670
T_{w2} - °F	731	640	632	659	655	752	750
T_{w3} - °F	735	666	651	678	670	768	772
T_{w4} - °F	750	680	667	708	706	794	787
T_{w5} - °F	750	686	672	717	702	792	785
T_{w6} - °F	688	622	607	634	609	692	713
T_{g1} - °F	713	629	638	652	638	720	728
T_{g2} - °F	734	640	653	666	659	752	-
T_{g3} - °F	743	647	666	680	676	777	795
T_{g4} - °F	763	658	676	704	711	802	807
T_{g5} - °F	753	650	667	702	710	790	792
T_{g6} - °F	753	666	669	700	701	763	774
T_{inlet} - °F	692	548	566	619	624	644	672
T_{outlet} - °F	672	619	641	594	619	687	748

Table IV

DATA FOR THE 15 INCH TEST SECTION

Temperatures at $\theta = \pi$

Run No.	23	24	25
V_o - ft./sec.	1.85	1.85	1.85
I - amps.	233	250	264
E - volts	1.94	2.08	2.30
(q/A)- Btu./hr.ft.^{2}	11400	13400	15400
T_f - °F	104	106	100
T_{w1} - °F	572	630	715
T_{w2} - °F	650	714	796
T_{w3} - °F	673	738	823
T_{w4} - °F	697	760	852
T_{w5} - °F	713	771	873
T_{w6} - °F	626	681	771
T_{g1} - °F	659	680	768
T_{g2} - °F	669	691	780
T_{g3} - °F	666	686	775
T_{g4} - °F	678	700	-
T_{g5} - °F	680	703	787
T_{g6} - °F	667	692	787
T_{inlet}- °F	532	540	582
T_{outlet}- °F	561	566	610

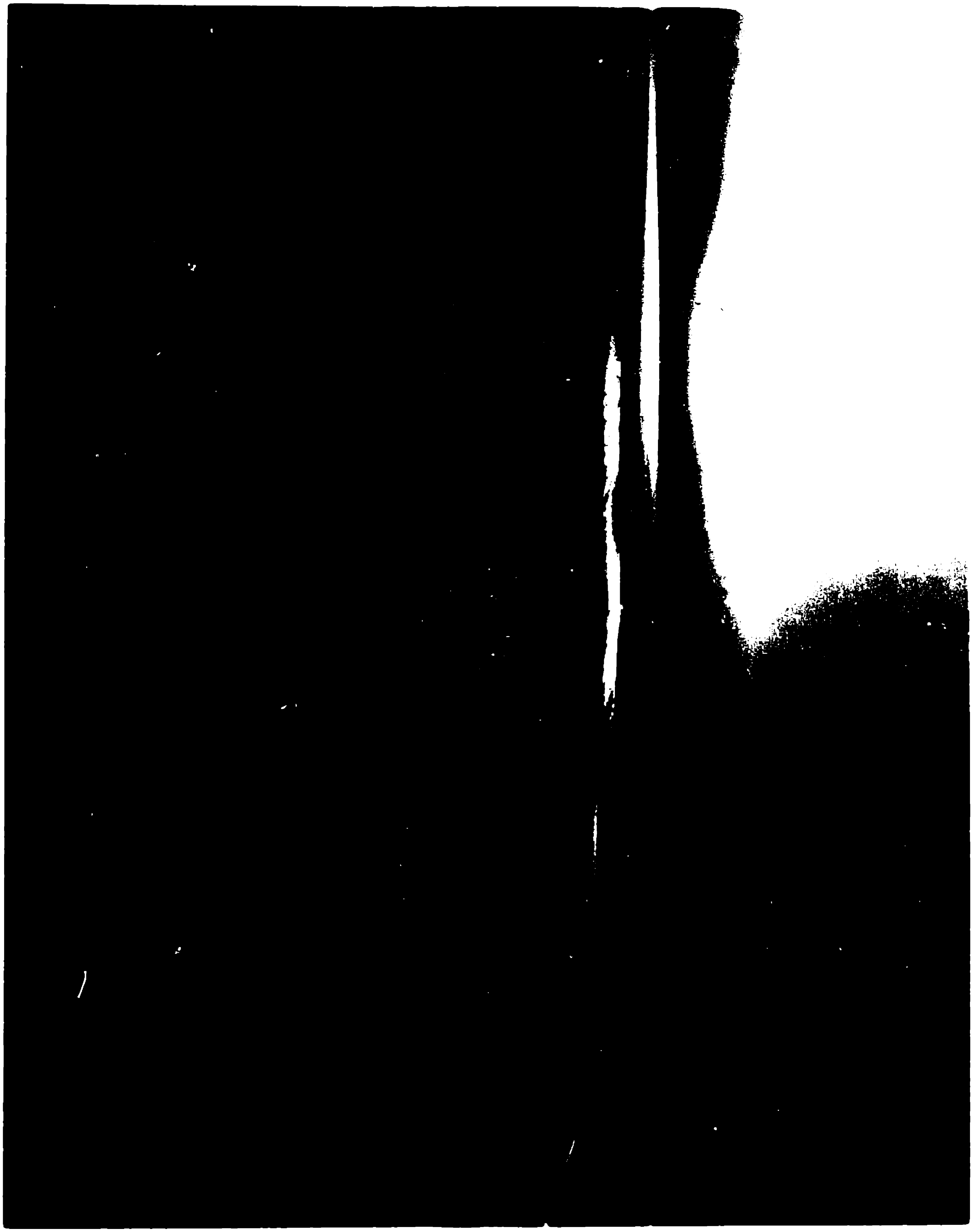

Figure 1 - Film boiling of Freon-113 in a horizontal tube with V_o = 1.85 ft/sec.

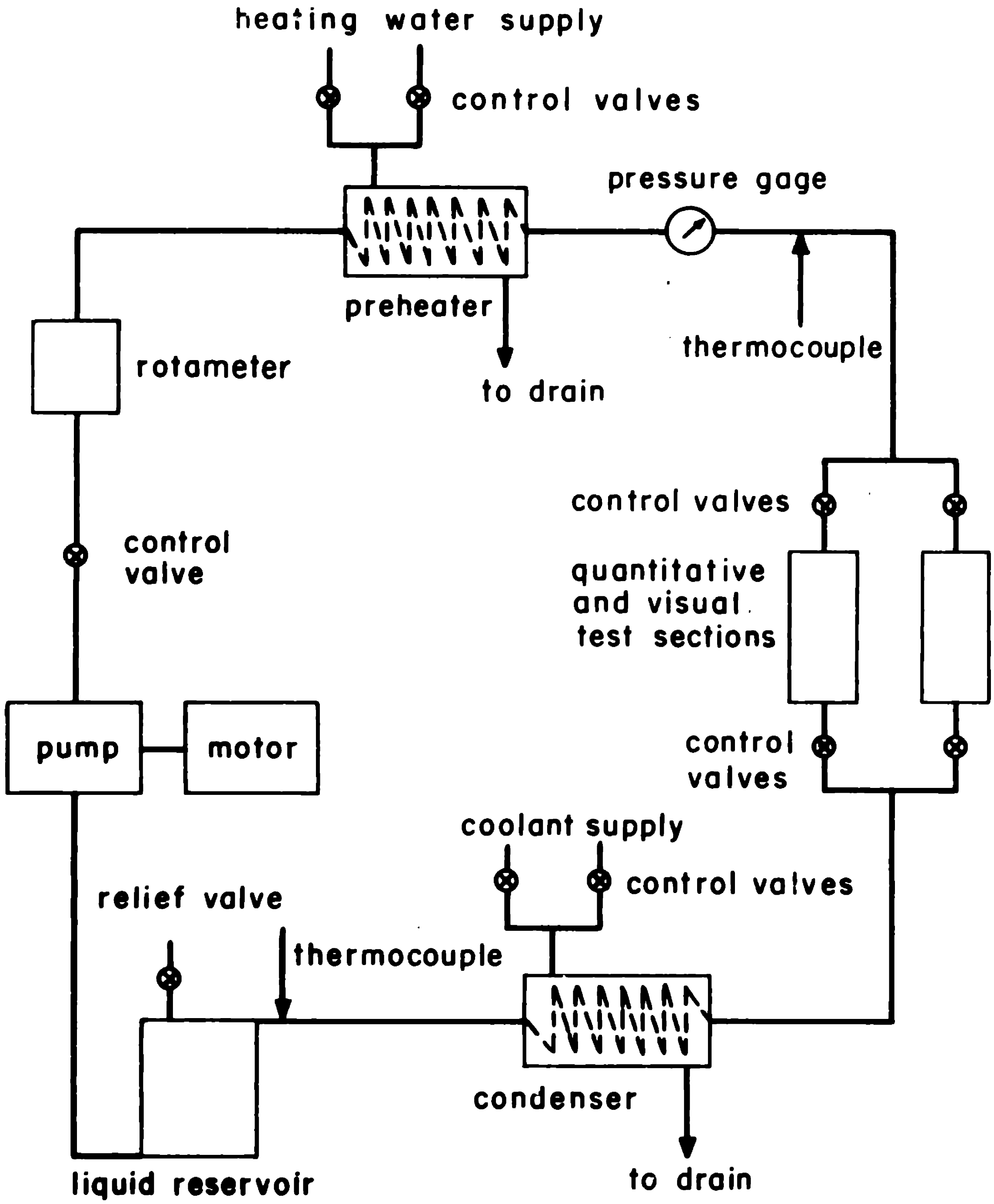

FIG. 2 SCHEMATIC DIAGRAM OF THE CIRCULATION SYSTEM

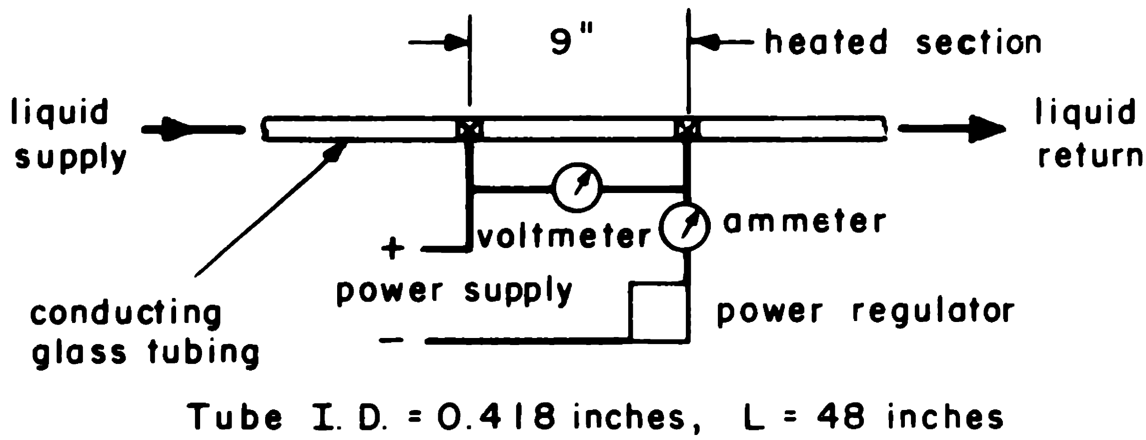

Fig. 3 SCHEMATIC DIAGRAM OF THE VISUAL TEST SECTION

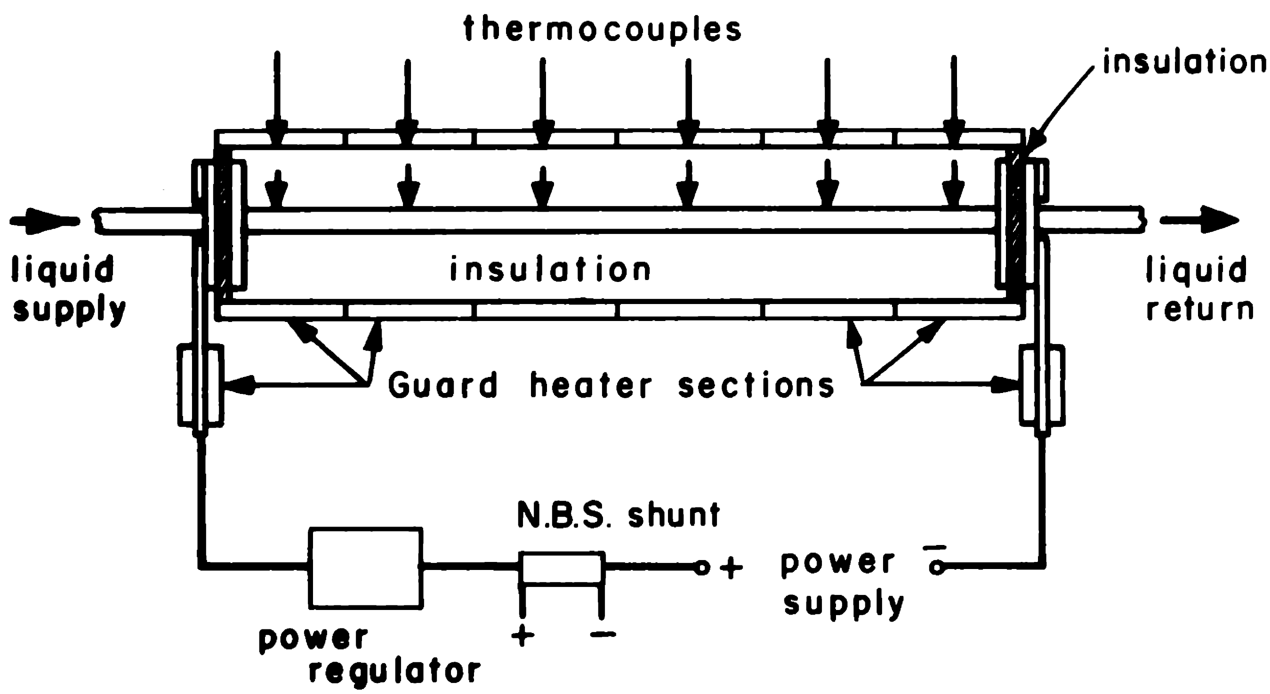

FIG. 4 SCHEMATIC DIAGRAM OF THE QUANTITATIVE TEST SECTION

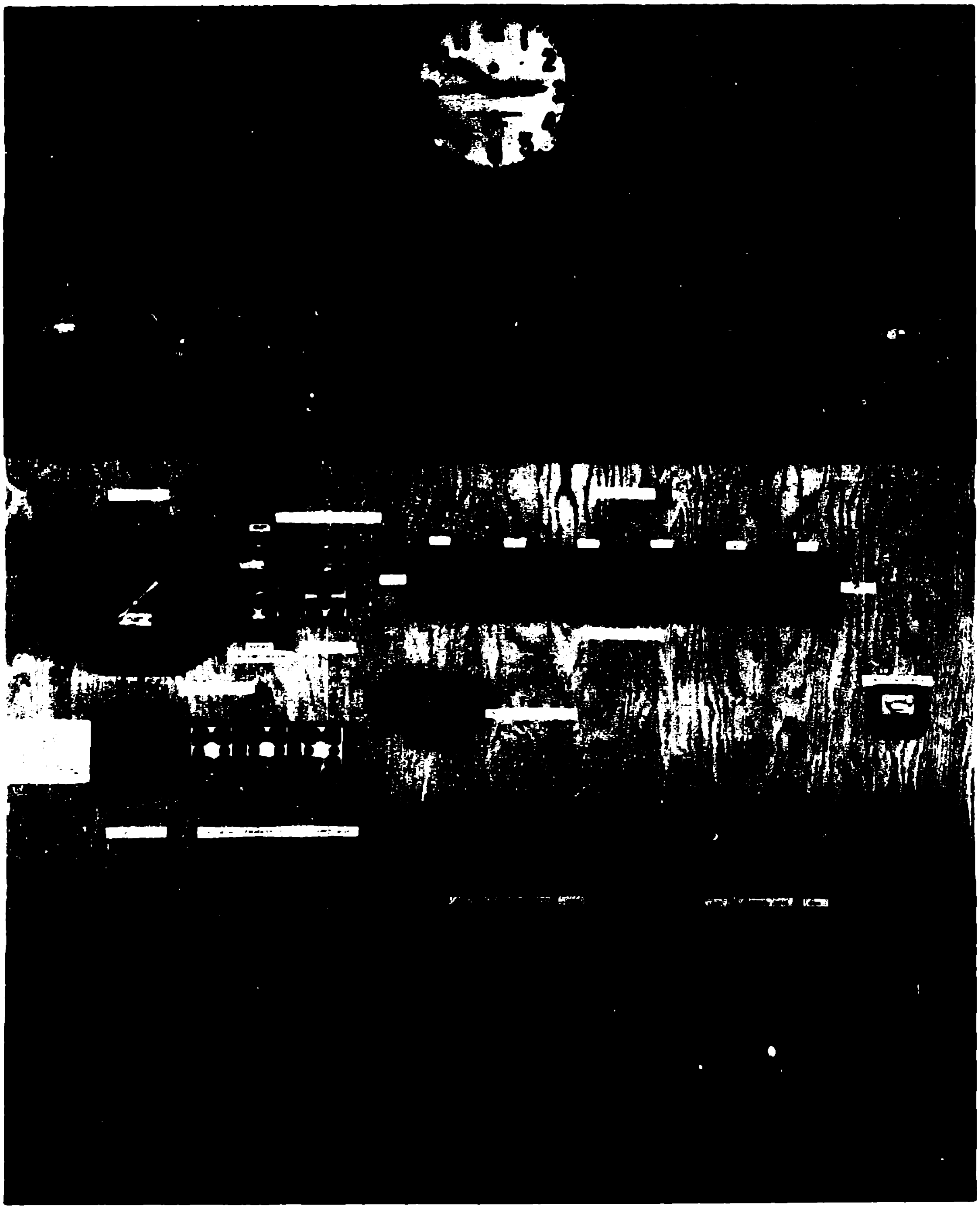

Figure 5 - Apparatus control panel and the visual test section

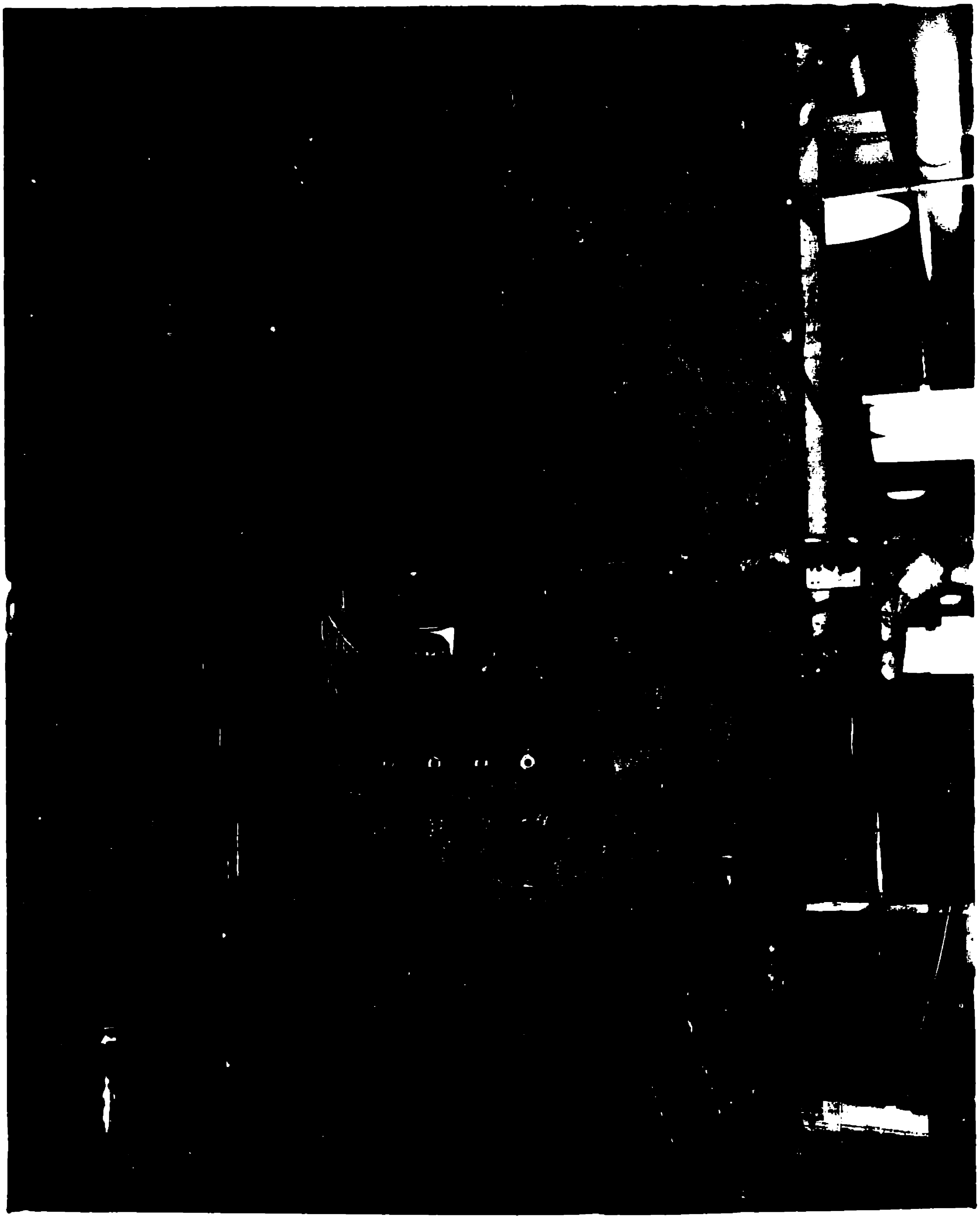

Figure 6 - Quantitative test section and parts of the control and circulation systems.

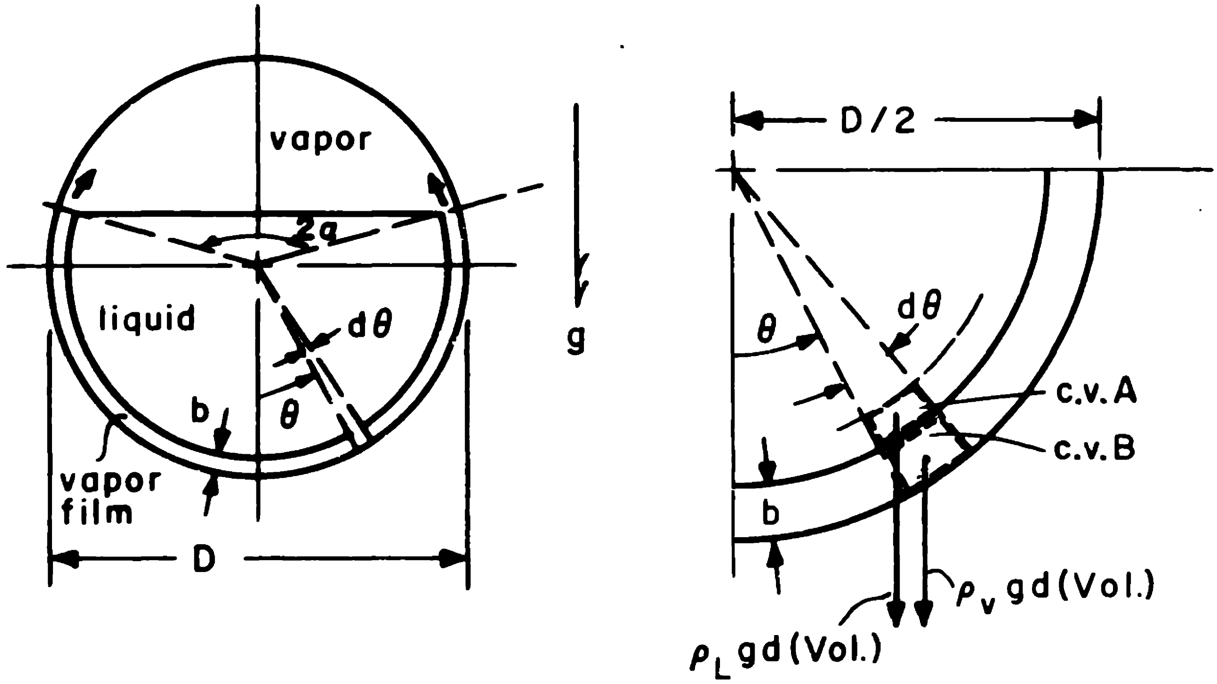

FIG. 7 CROSS SECTION OF IDEALIZED FLOW MODEL

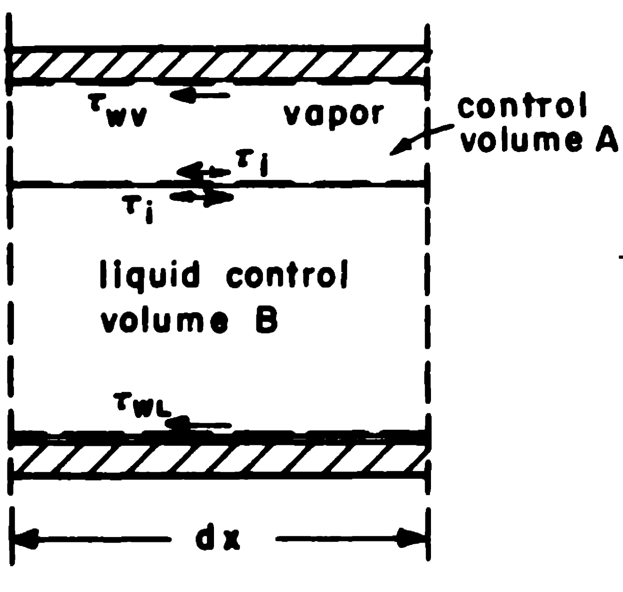

FIG. 8 GEOMETRY FOR MOMENTUM ANALYSIS

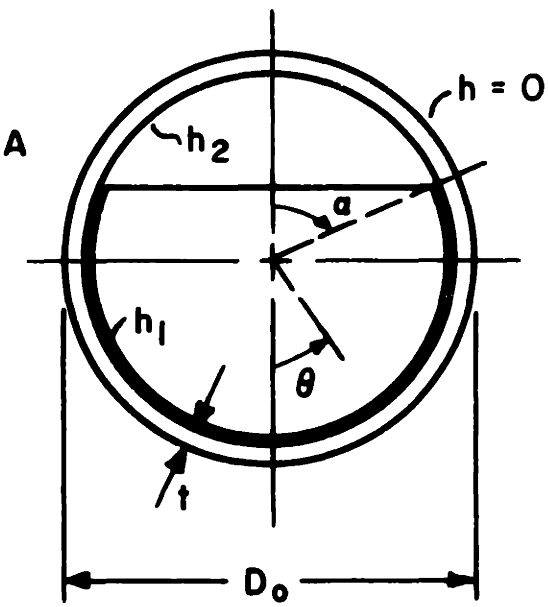

FIG. 9 GEOMETRY FOR CONDUCTION ANALYSIS

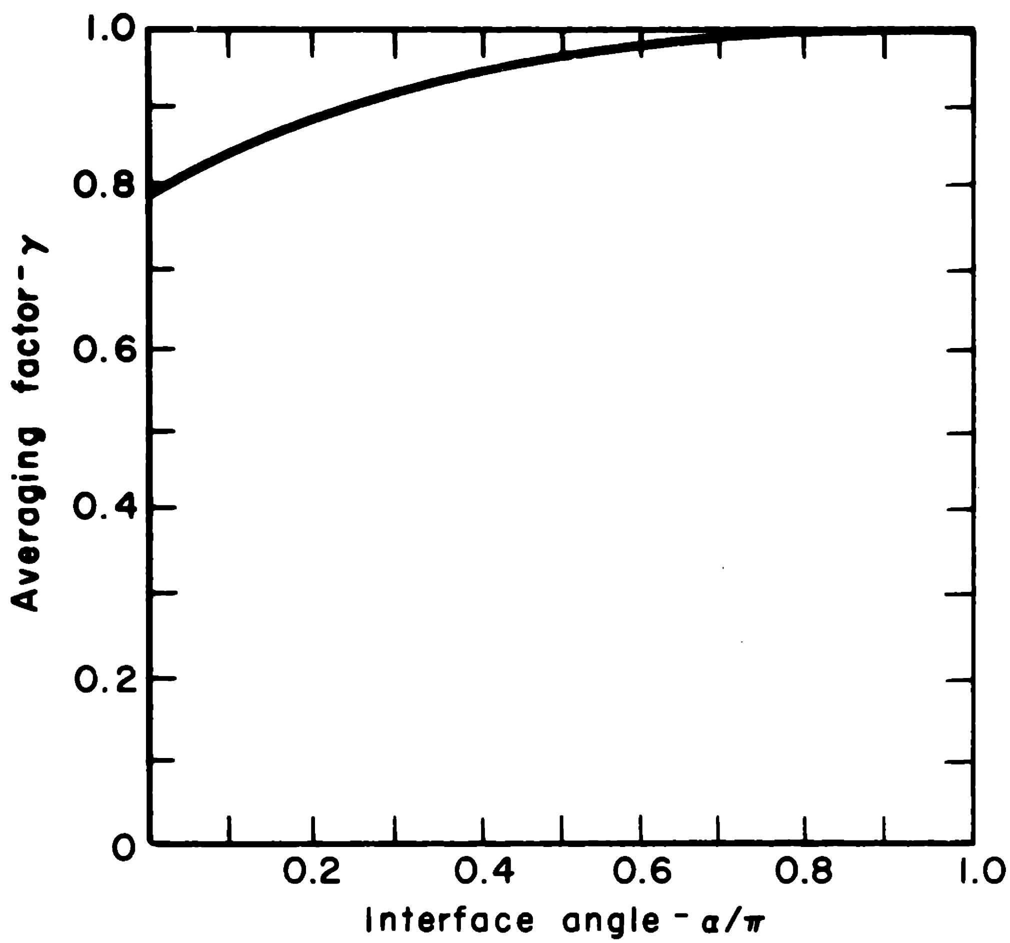

FIG. 10 BOILING HEAT TRANSFER COEFFICIENT MULTIPLIER, γ vs. α/π

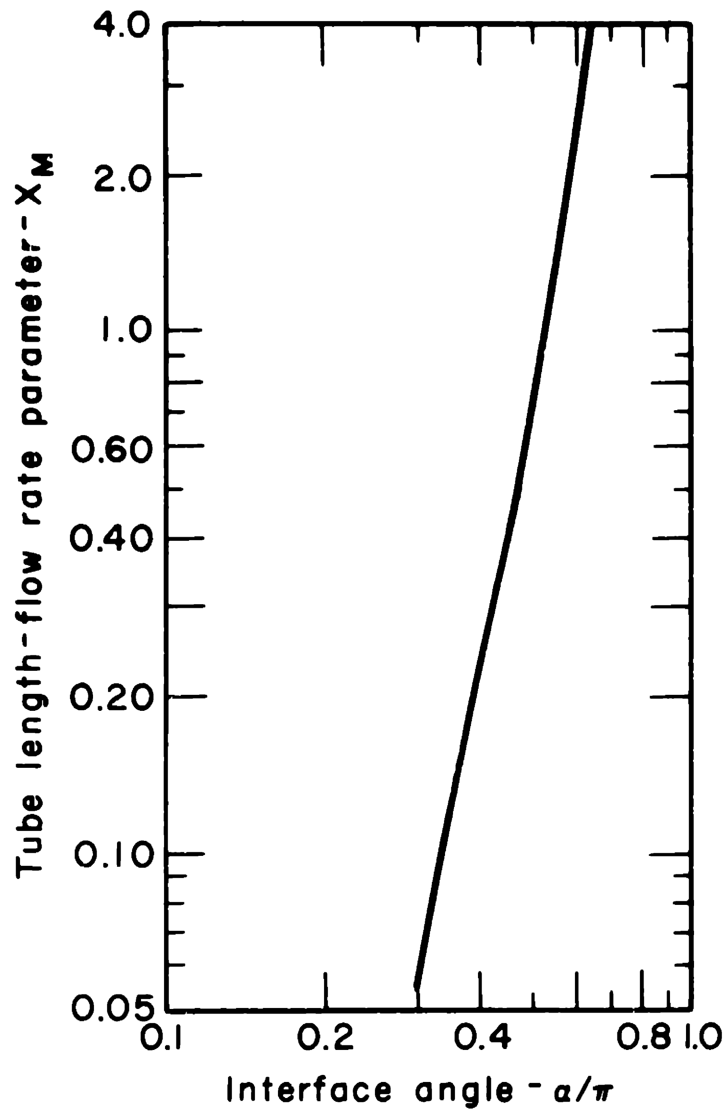

FIG. 11 TUBE LENGTH - FLOW RATE PARAMETER vs. α/π

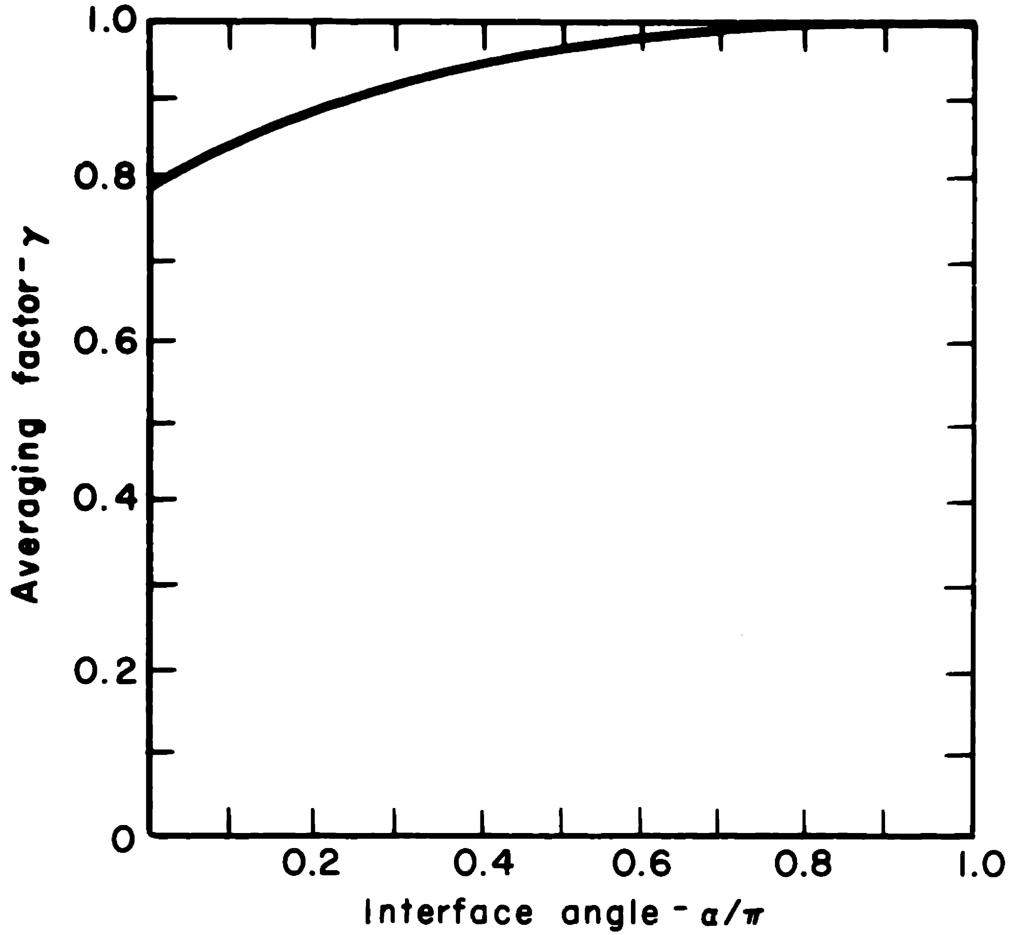

FIG. 10 BOILING HEAT TRANSFER COEFFICIENT MULTIPLIER, γ vs. a/π

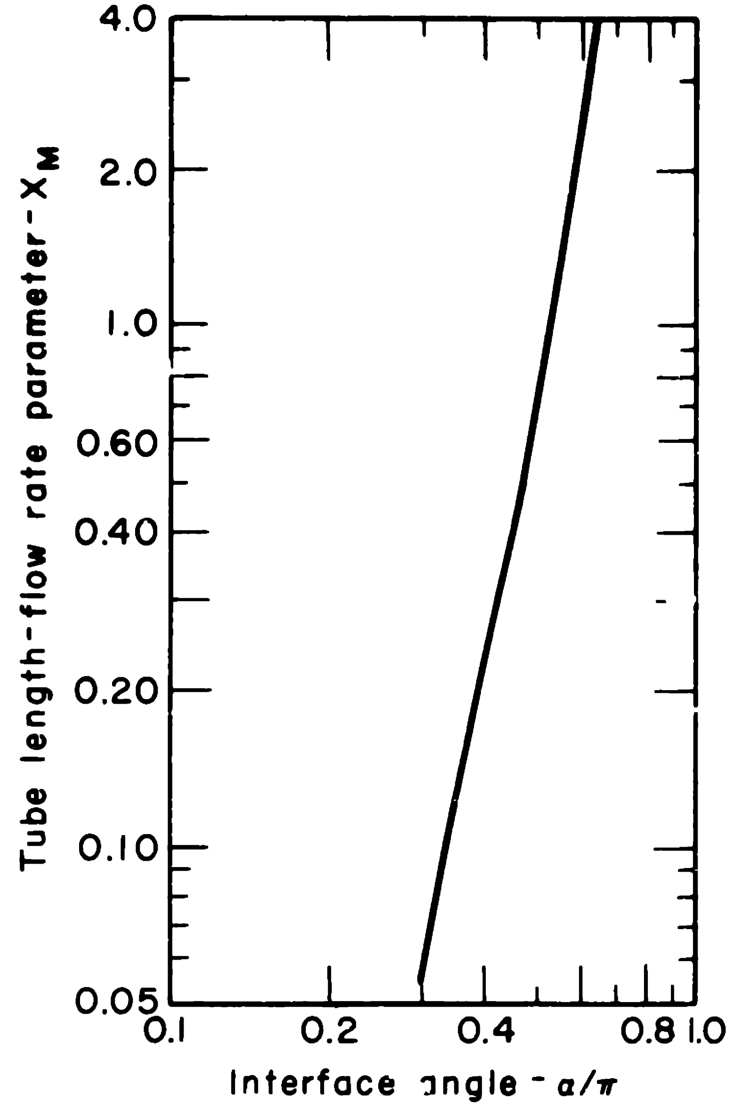

FIG. 11 TUBE LENGTH - FLOW RATE PARAMETER vs. a/π

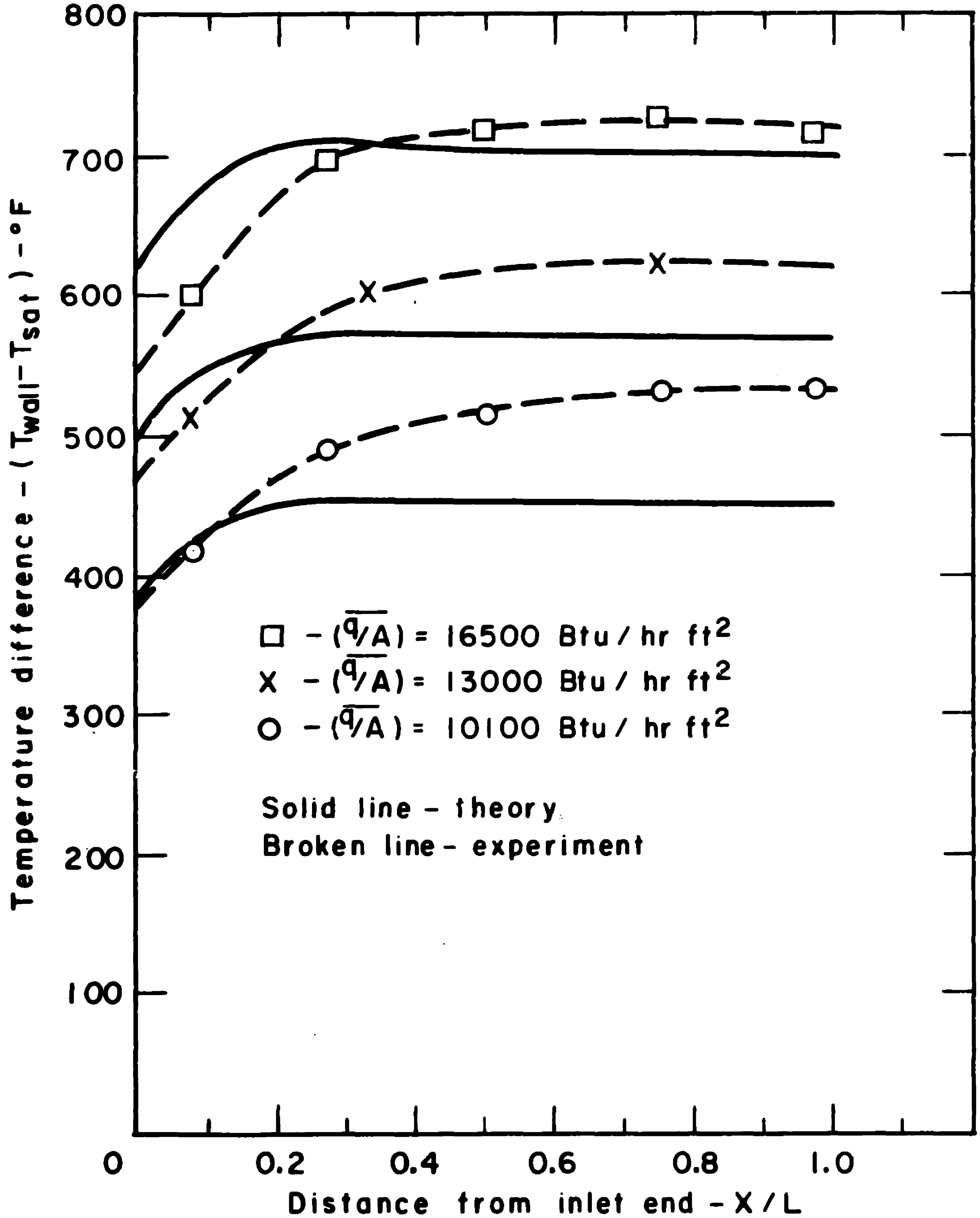

FIG. 12 TEMPERATURE DISTRIBUTION WITH X/L FOR V_o = 1.23 ft/sec AND θ = 0

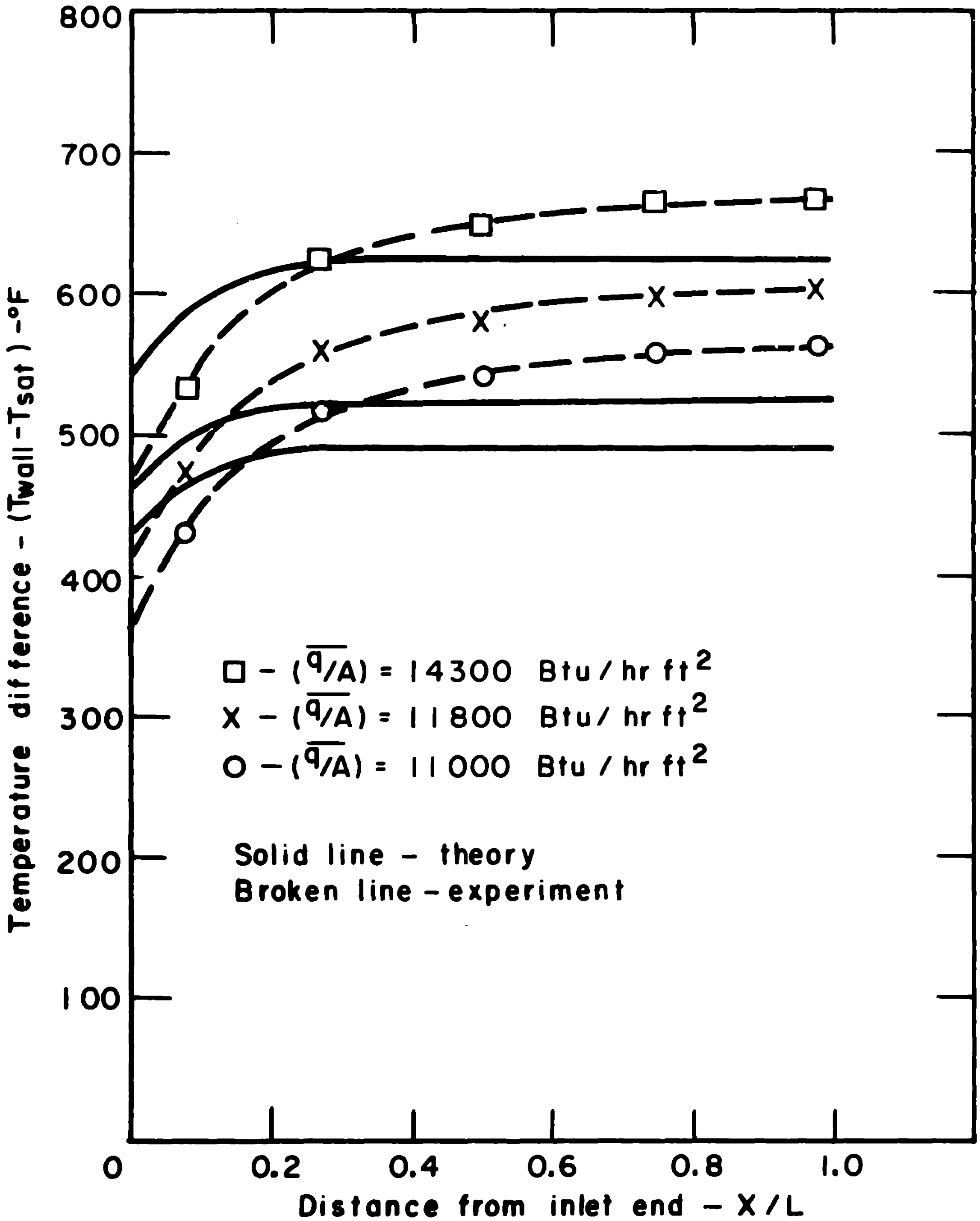

FIG. 13 TEMPERATURE DISTRIBUTION WITH X/L FOR $V_0 = 1.23$ ft/sec AND $\theta = 0$

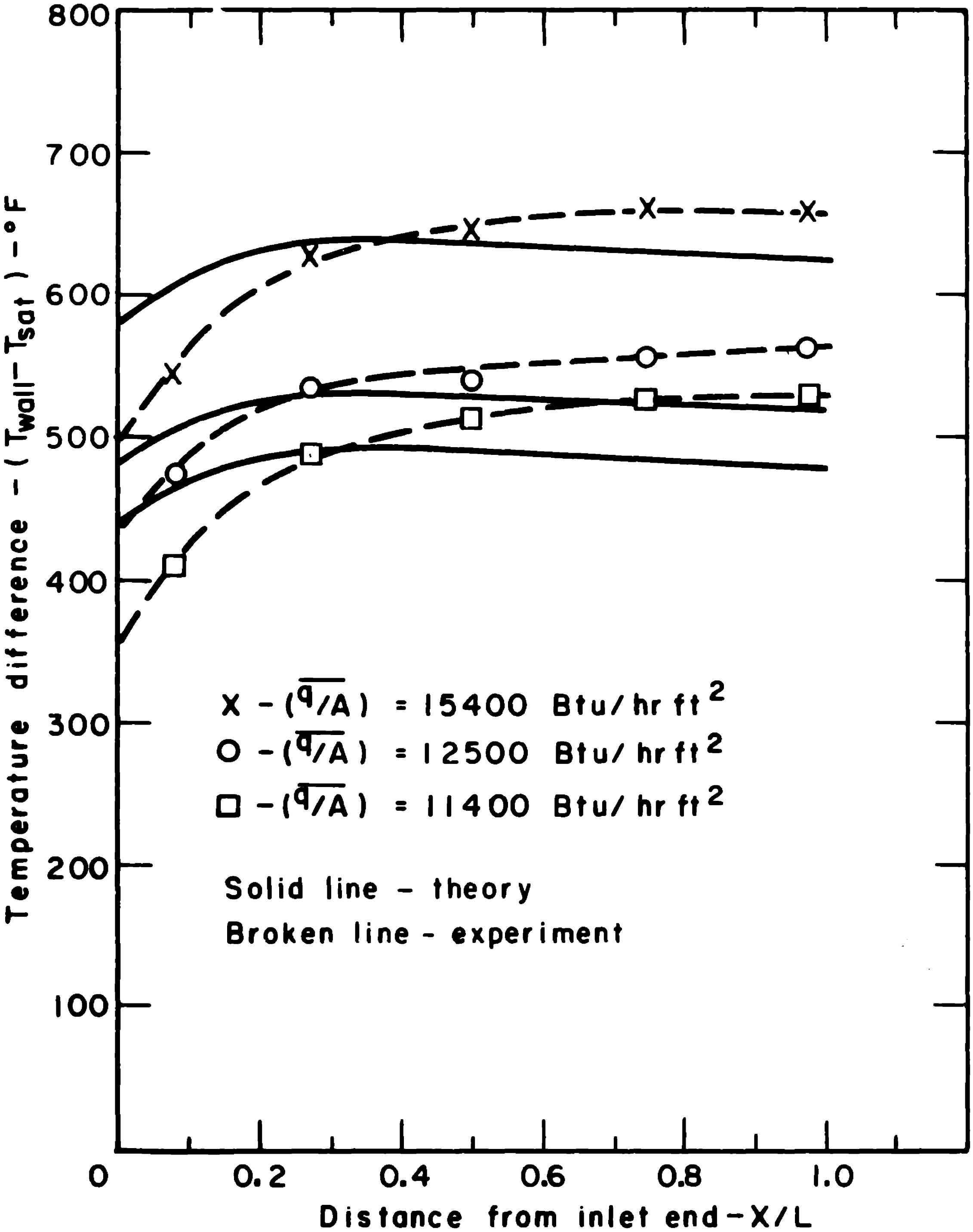

FIG. 14 TEMPERATURE DISTRIBUTION WITH X/L FOR V_0 = 1.85 ft/sec AND θ = 0

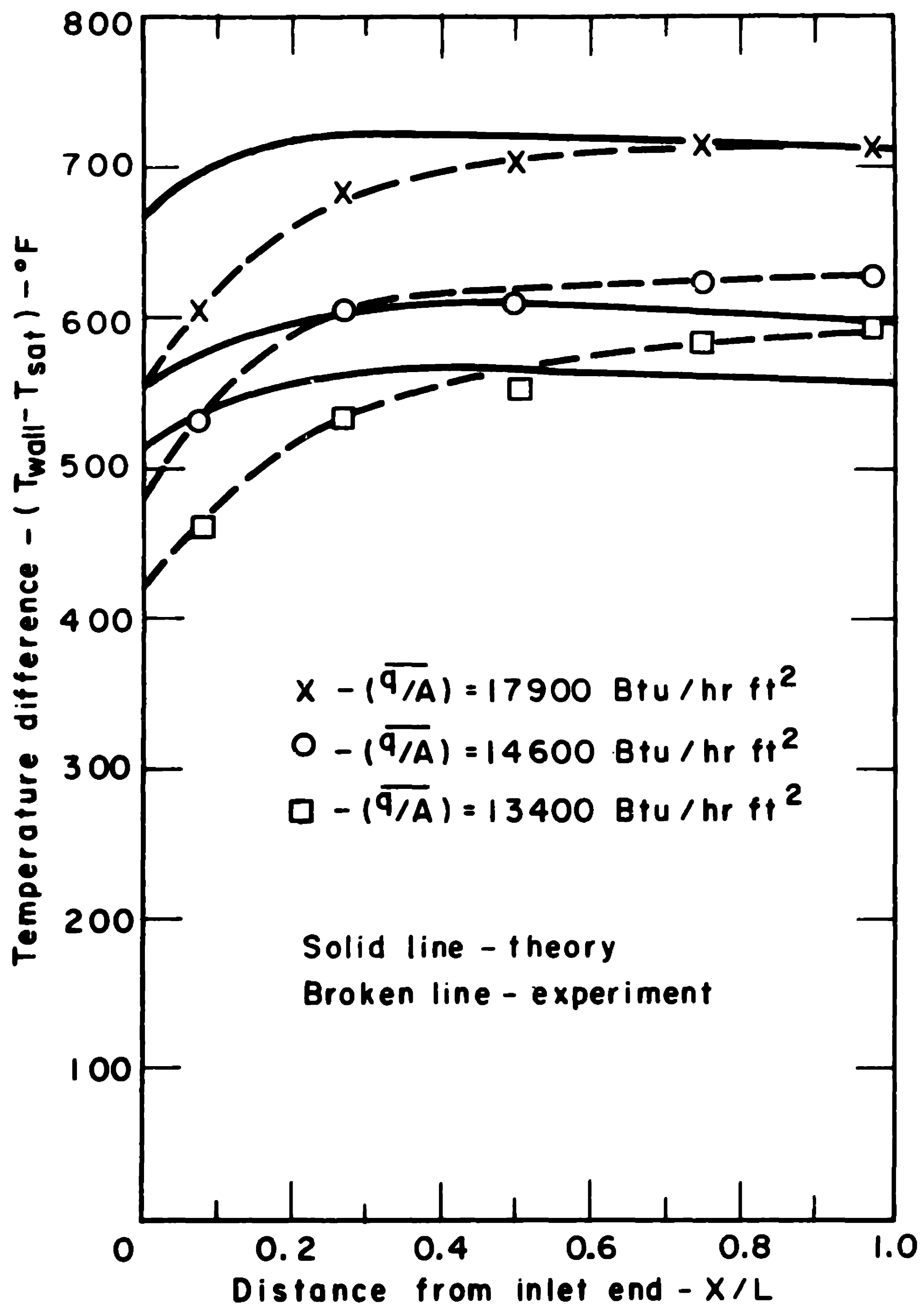

FIG. 15 TEMPERATURE DISTRIBUTION WITH X/L FOR V_0 = 1.85 ft/sec AND θ = 0

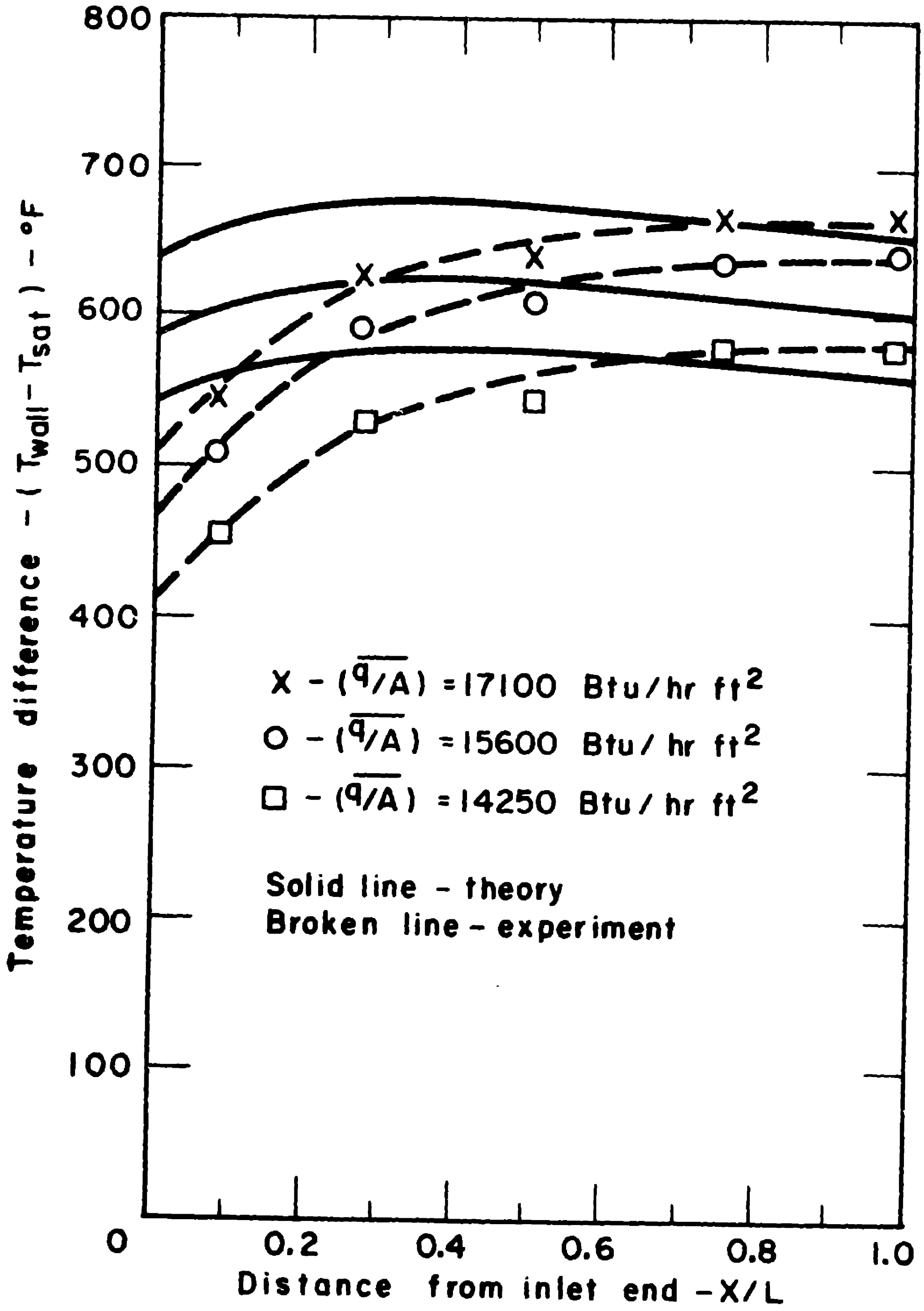

FIG. 16 TEMPERATURE DISTRIBUTION WITH X/L FOR V_0 = 2.46 ft/sec AND θ = 0

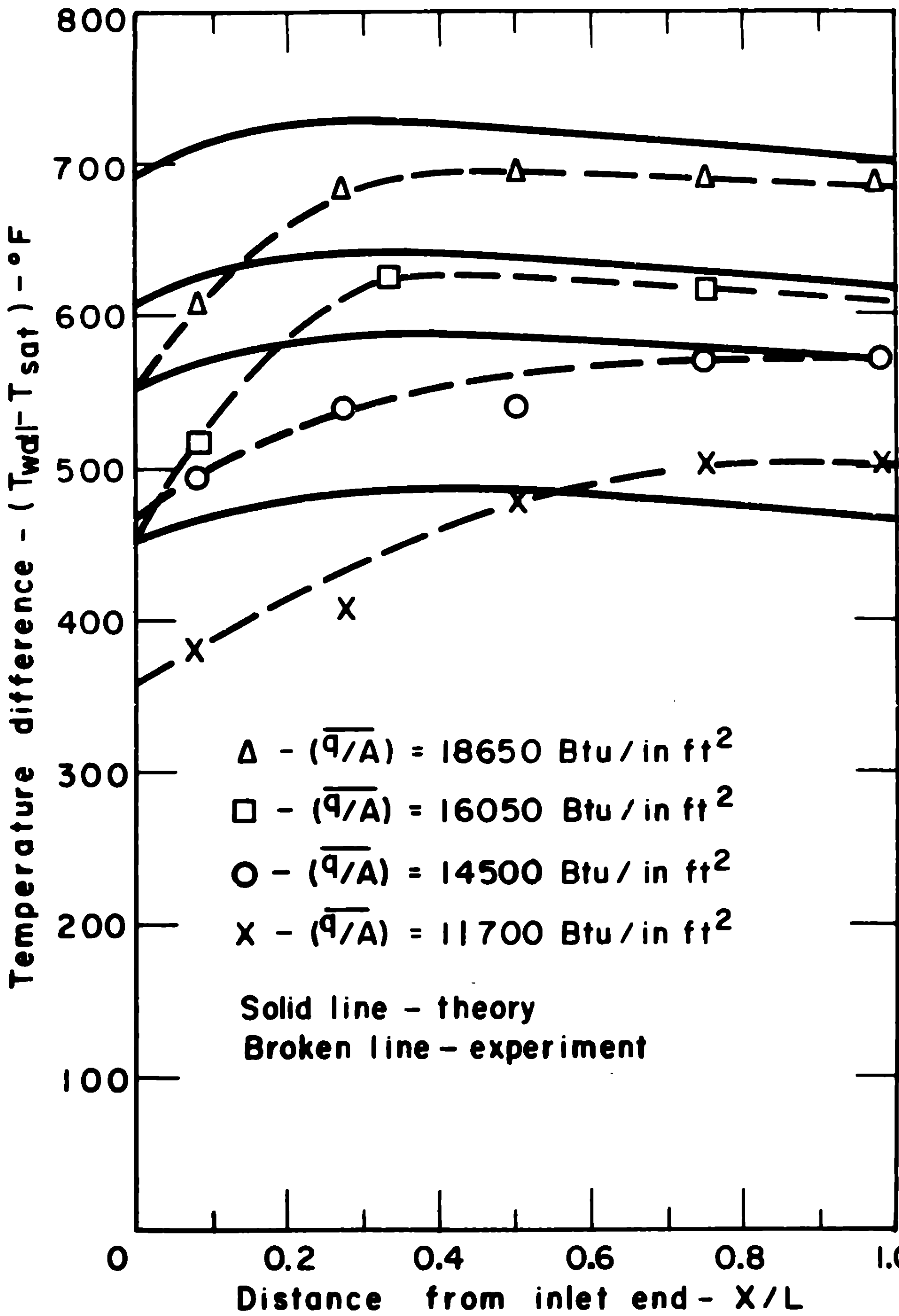

FIG. 17 TEMPERATURE DISTRIBUTION WITH X/L FOR $V_0 = 2.46$ ft/sec AND $\theta = 0$

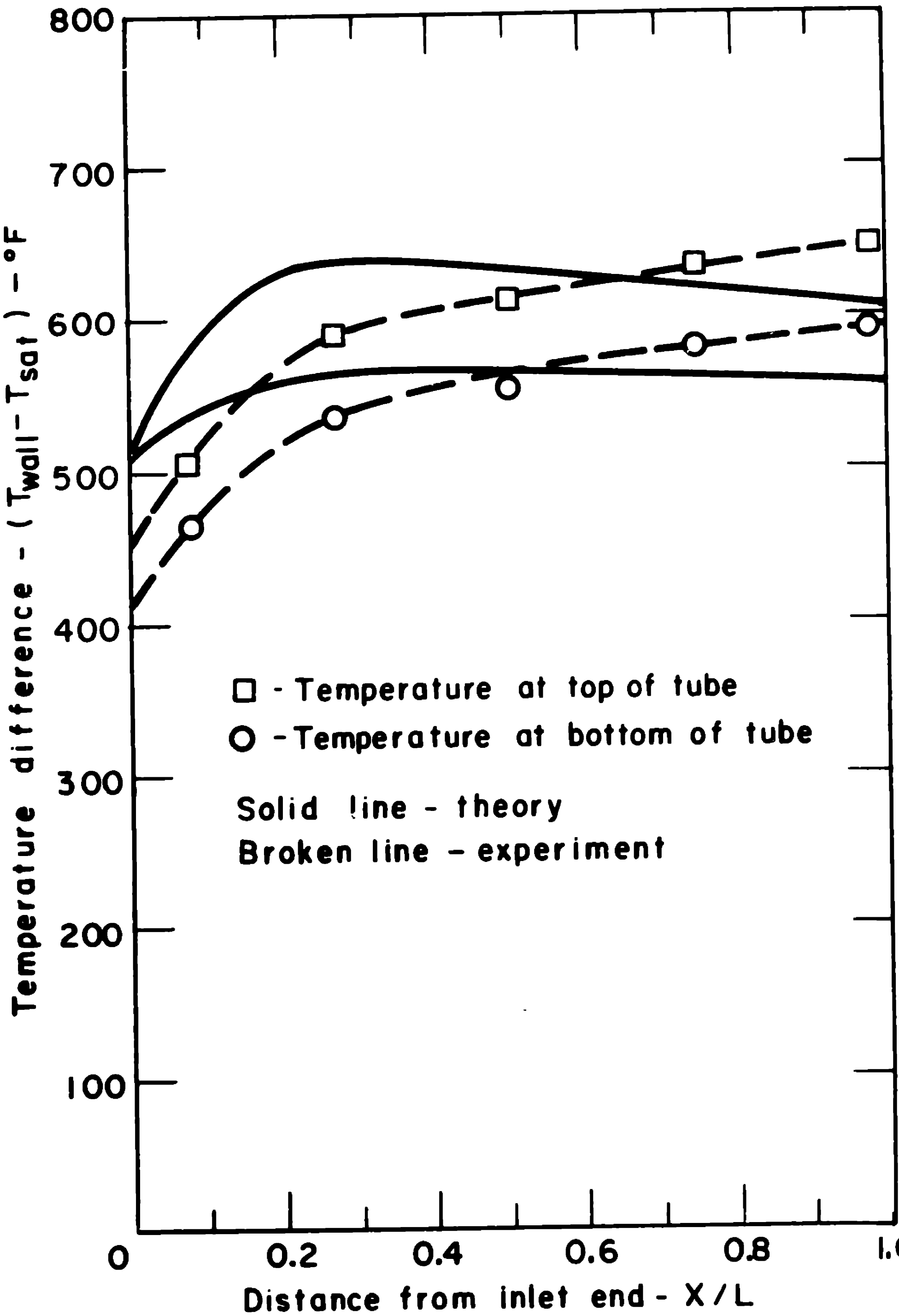

FIG. 18 TEMPERATURE DISTRIBUTION AT $\theta = \pi$ AND $\theta = 0$ FOR $V_0 = 1.85$ ft/sec AND $(q/A) = 13400$ Btu/hr ft^2

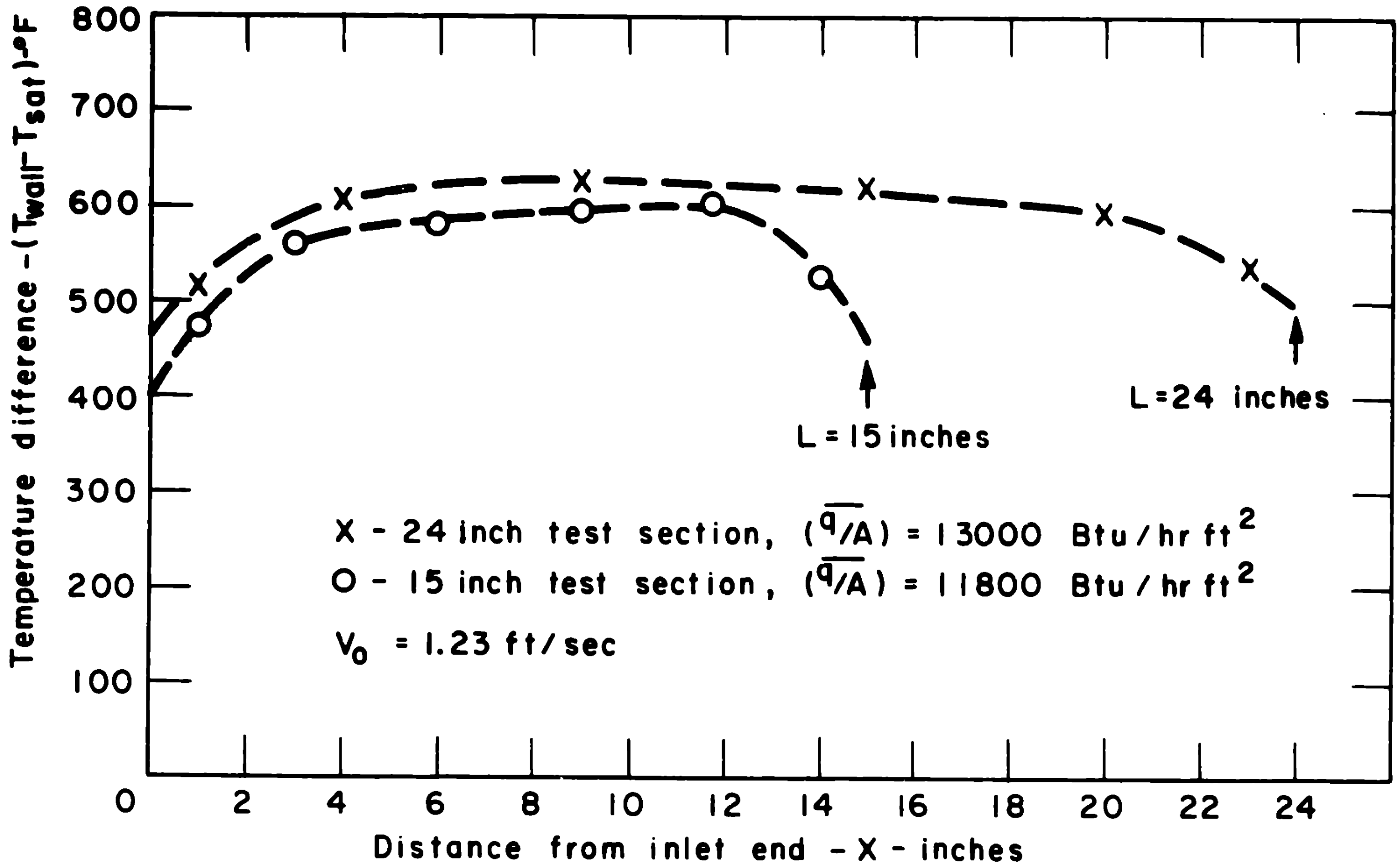

FIG. 19 COMPARISON OF DATA FOR DIFFERENT TEST SECTION LENGTHS

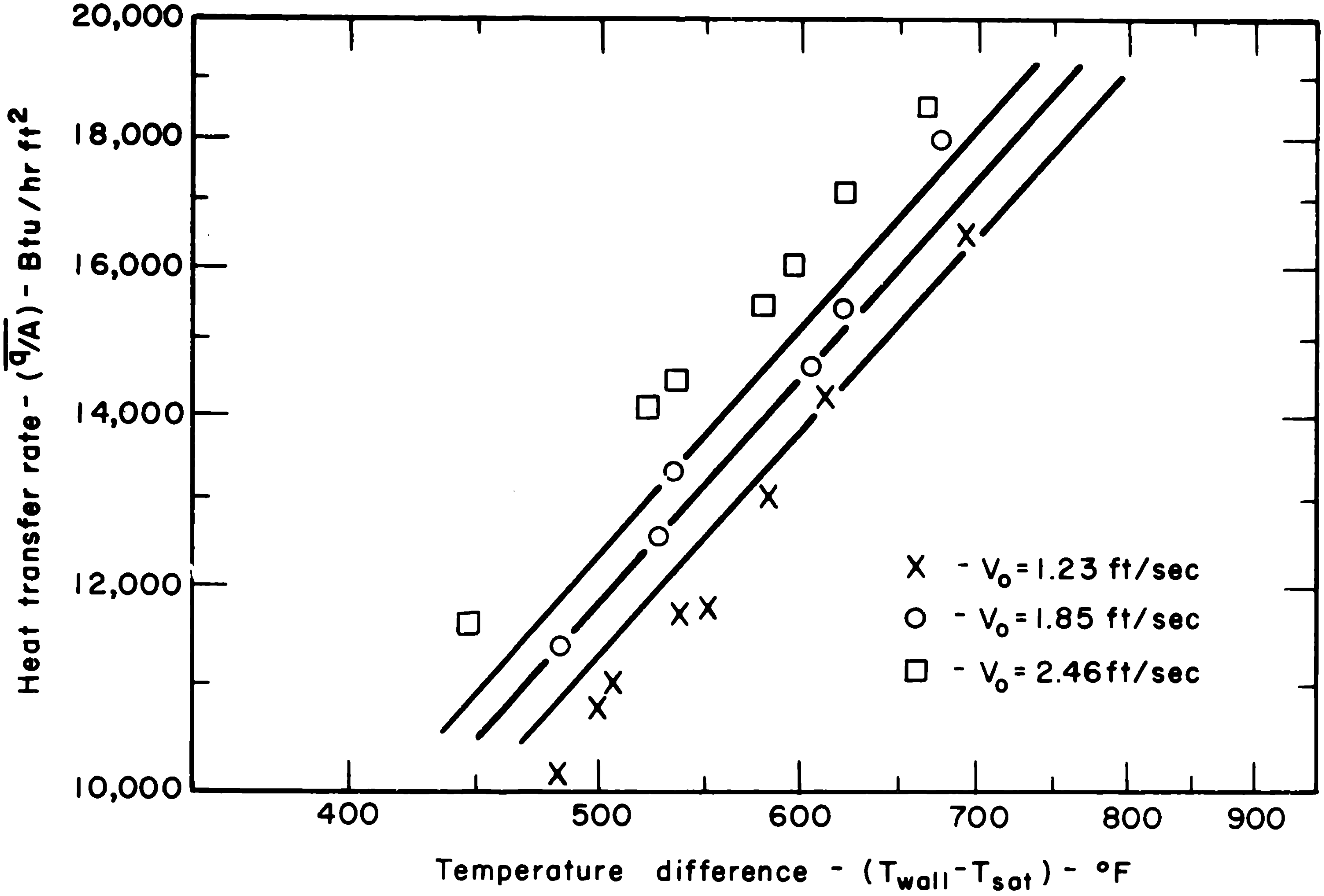

FIG. 20 HEAT FLUX vs. TEMPERATURE DIFFERENCE AT X/L=0.25

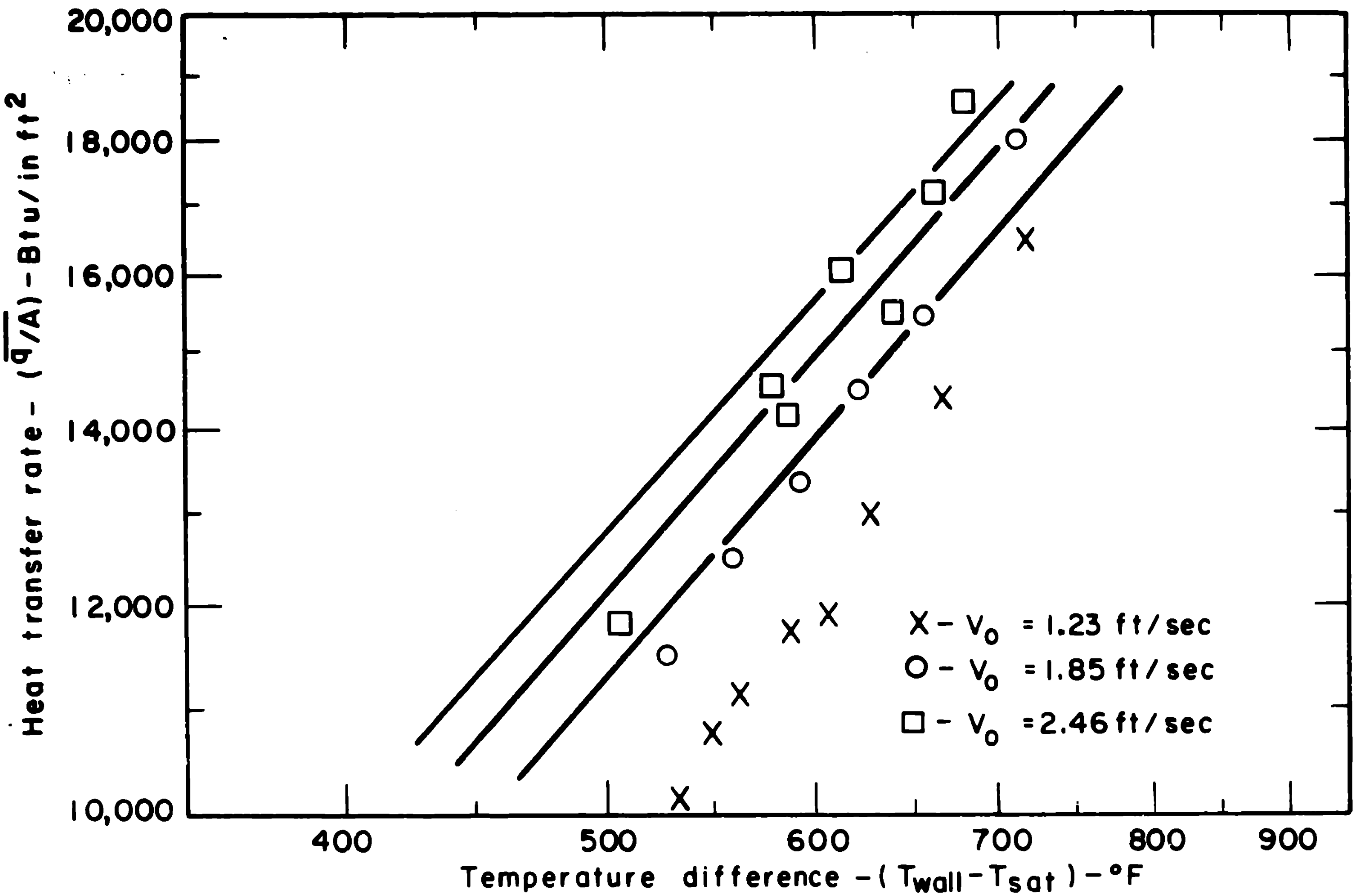

FIG. 21 HEAT FLUX VS. TEMPERATURE DIFFERENCE AT X/L = 1.0

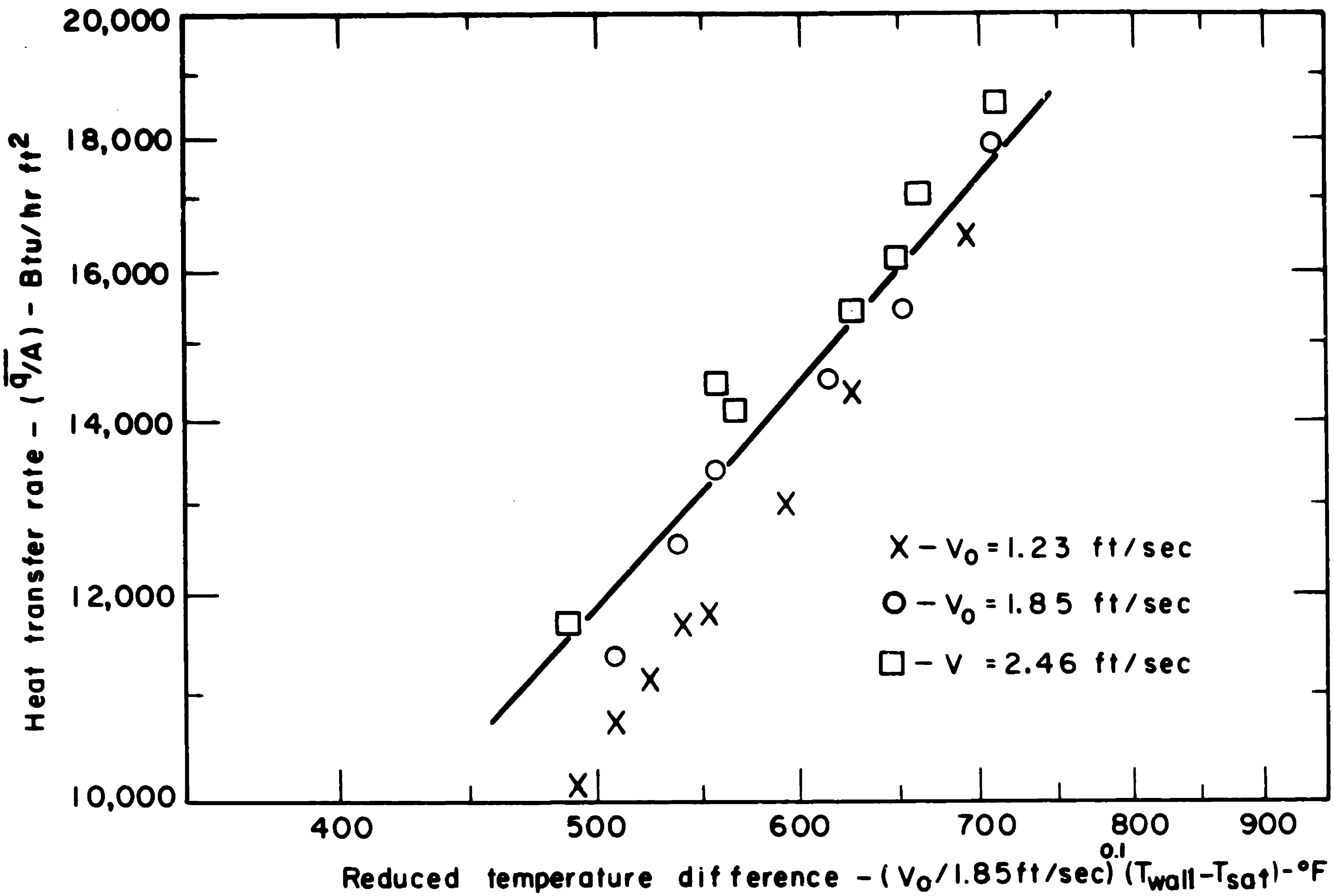

FIG. 22 HEAT FLUX VS REDUCED TEMPERATURE DIFFERENCE AT X/L = 0.5